8-2017

Geophysical Assessment of Kinion Lake Dam

Tim Allen Moody
University of Arkansas, Fayetteville

Geophysical Assessment of Kinion Lake Dam

A thesis submitted in partial fulfillment
of the requirements for the degree of
Master of Science in Civil Engineering

by

Tim Moody
University of Arkansas
Bachelor of Science in Civil Engineering, 2015

August 2017
University of Arkansas

This thesis is approved for recommendation to the Graduate Council

Dr. Clinton M. Wood
Thesis Director

Dr. Michelle Bernhardt
Committee Member

Dr. Gary Prinz
Committee Member

Abstract

Geophysical methods including Capacitively-Coupled Resistivity (CCR), Electrical Resistivity Tomography/Imaging (ERT/ERI), Multichannel Analysis of Surface Waves (MASW) with Love and Rayleigh waves and a Full-Waveform Inversion (FWI) were performed on Kinion Lake Dam, an earth-filled embankment dam that has historically experienced significant seepage and internal erosion issues. Surveys were completed along the crest and downstream toe of the dam. Results from the surveys indicate that each method is capable of resolving the bedrock depth within 1-2 m of locations shown on previous drilling logs, though some discrepancies between the methods exist. A weathered bedrock layer is believed to have led to the different depths between the methods. Rayleigh wave MASW and FWI were determined to be most effective at determining bedrock depth at deeper bedrock locations (i.e., the dam crest) and Love wave MASW was the only viable seismic method at detecting bedrock for areas with thin soil layers and complex bedrock geometry (i.e., the dam toe). The CCR and ERI results were in general agreement in bedrock depth estimation except for a long region in the middle of the dam, which assuming temporal water level variation, is an area of potential internal erosion. Higher water levels when the CCR data was collected in the spring are believed to have resulted in lower resistivities, due to the presence of water, while lower summer water levels resulted in higher resistivities for the ERI results, suggesting that fines may have been eroded out of the interior of the dam over time. This indicates that both CCR and ERI provide consistent data and demonstrates the importance of resistivity monitoring or seasonal surveys for internal erosion detection. The use of these resistivity methods also successfully detected a potential seepage path along the downstream toe of the dam where large seeps occur during large precipitation events.

Table of Contents

Table of Figures

1 Introduction

Geophysical testing is the use of a physical property of the subsurface materials to explore that subsurface and allow its characterization. Geophysical testing is appropriate for infrastructure evaluation for several reasons: it is generally non-destructive resulting in little or no damage to the infrastructure being evaluated, it is rapid in execution allowing large distances to be surveyed relatively quickly, and the tests return results that can be used to perform engineering evaluations of the tested infrastructure. Wave-based geophysical testing has become an increasingly popular method to obtain engineering information about the subsurface. These wave-based methods take the form of either electromagnetic waves, measuring electrical resistance, or stress waves, measuring stiffness, each with their own strengths and weaknesses.

1.1 Electrical Resistivity Methods

Electrical resistivity methods work by inducing a current into the ground and measuring the resulting voltage at differing distances. By varying the transmitting electrode and potential electrode distances, the current travels through different subsurface paths at different depths allowing the resistivity of the subsurface to be characterized (Loke, 1999). The resistivity of a material is a measure of how strongly that material resists the flow of electrical current. These techniques are based on the correlation of resistivity with the type of material and is strongly influenced by the presence of water in the material. The ranges of resistivity corresponding to various materials consist of clays and shales at the less resistive end (10 – 100 Ω-m), gravels, sands and rock at the highly resistive end (800+ Ω-m), and silts and porous sedimentary rock in the middle (80-1000 Ω-m) (Palacky, 1987). However, the presence of water in more porous materials can make it much more difficult to interpret particular resistivity values as particular materials confidently. Rein, Hoffman, and Dietrich (2004) performed a long-term direct current

(DC) resistivity monitory survey at two test sites to determine what site parameters most significantly affect resistivity measurements, concluding that water saturation, soil temperatures, groundwater temperatures, and groundwater ion concentrations also affected resistivity measurements the most in decreasing significance.

Traditional DC resistivity surveys were developed in the 1920's by the Schlumberger brothers to detect metal deposits and generally consist of four, collinear electrodes arranged in one of three configurations. The Schlumberger array, shown in Figure 1-1a, uses the outer two electrodes to complete the circuit and the internal distance to the two potential electrodes is varied to increase survey depth. Similarly, the Wenner array, shown in Figure 1-1b, uses the outermost electrodes to complete the circuit, however, all four electrodes are kept equidistant, requiring all four to be moved for deeper surveys, unlike in a Schlumberger array. Despite the longer testing time, Wenner arrays have been found to have the best signal response and horizontal resolution, though a more limited depth of investigation (Seaton & Burbey, 2002).

The third configuration is the dipole-dipole, shown in Figure 1-1c, in which the two current-bearing electrodes are adjacent to one another and spaced equally to the potential measuring electrodes. The distance between these pairs can be varied to increase survey depth. Dipole-dipole arrays are more susceptible to noise, have lower signal-to-noise ratios, have better resolution particularly for dipping layers, and somewhat less depth resolutions than the alternatives (Dahlin & Bing, 2004).

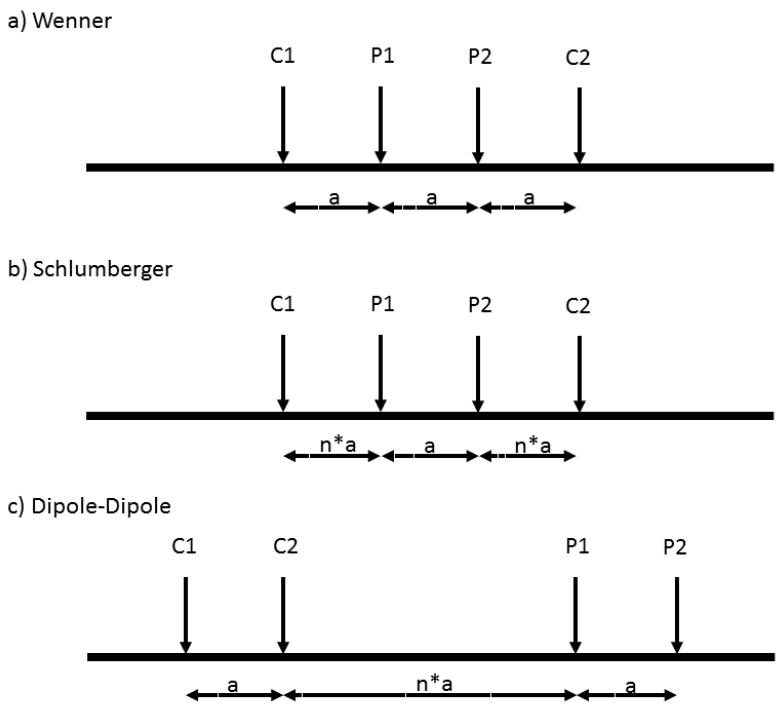

Figure 1-1. DC array configurations: a) Wenner, b) Schlumberger, c) Dipole-Dipole.

2D DC surveys, also known as electrical resistivity imaging (ERI) allow continuous resistivity profiling along infrastructure like levees, dams, and roads. The typical setup consists of steel stakes attached to electrode cables connected to a resistivity meter, allowing long arrays of electrodes to induce current and measure potential in a semi-automated manner, proceeding from smallest spacing to largest, shown in Figure 1-2. The entire staked array can then be moved forward, resulting in longer 2D profiles. Alternatively, multiple electrode cables can be used in a line and once one set of electrodes is no longer needed, it can be moved to the end, extending the survey distance, as seen in Figure 1-3 (Dahlin, 1996). This reliance on computer-controlled multiple electrode systems allows much faster data collection over larger areas.

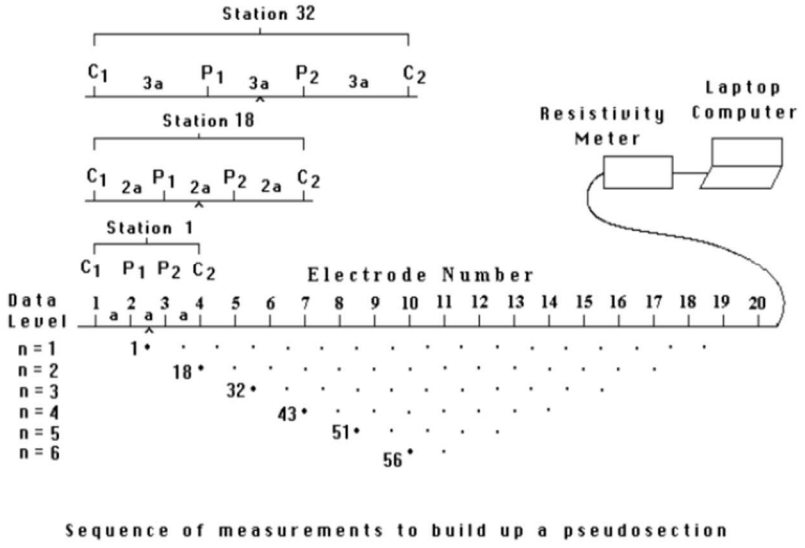

Figure 1-2. Using a set of electrodes and cables to survey at different depths by varying the spacing (Loke, 1999).

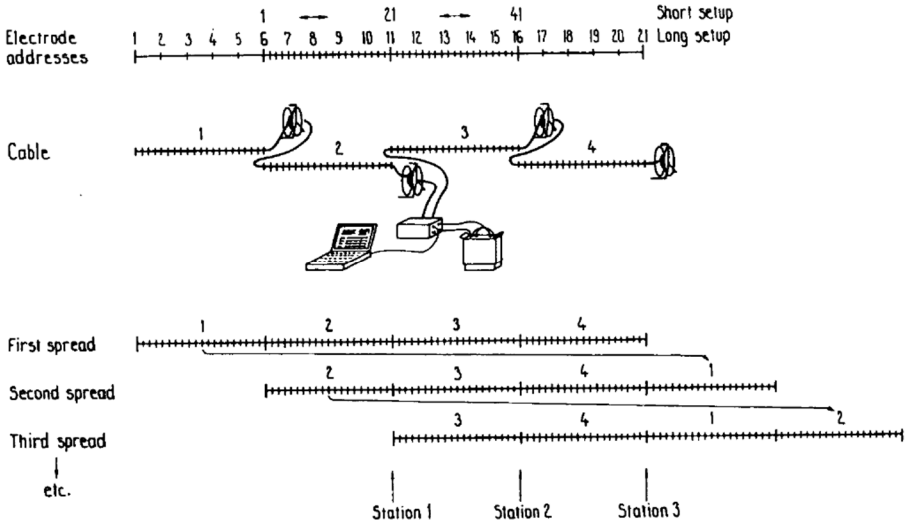

Figure 1-3. ERI roll-along schematic (Dahmin, 1996).

Capacitively-coupled resistivity methods (CCR) solve many of the limitations inherent in traditional DC surveys by not requiring electrodes staked into the ground. In ERI surveys, this staking requirement makes testing pavements, gravelly surfaces, frozen terrain, and well compacted soils very difficult or even impossible. DC surveys also have difficulty with high

surface resistivity values found on those same terrain types (Baines, et al., 2002). CCR uses a transmitter and receivers coupled in a dipole-dipole configuration. Using line antennas, these electrodes can be dragged along the ground, shown in Figure 1-4, as a single unit enabling very rapid measurements over large distances (Timofeev, et al., 1994).

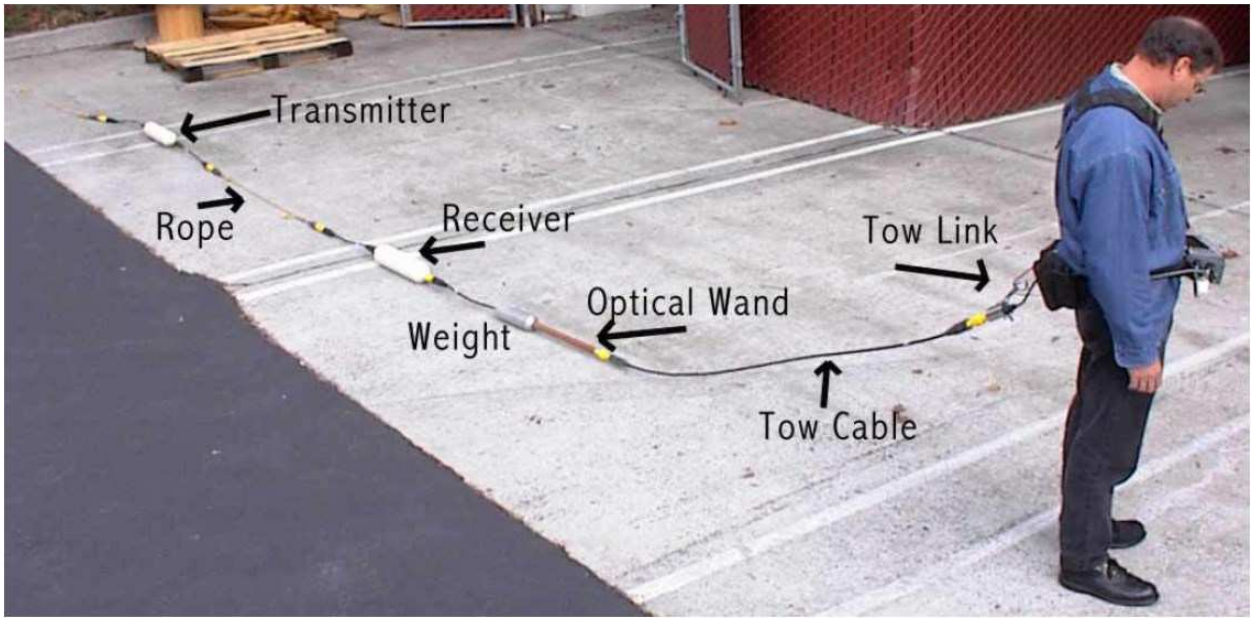

Figure 1-4. Geometrics OhmMapper (Dipole-Dipole CCR configuration) towing setup (Geometrics, 2001).

Obtaining a subsurface resistivity model requires first creating a pseudosection profile. This is normally done by locating an apparent resistivity value at the midpoint of the transmitter and the receiver and at a depth proportional to the distance between the two. The resulting pseudosection only approximates the true resistivity distribution below the surface and is mostly used to identify and remove unusually large or low values (Loke, 1999). After processing a pseudosection, a subsurface model can be obtained by use of a forward modeling program using either finite-difference or finite-element methods. In geophysical inversion problems, there exist infinite possible solutions that can result in the same apparent resistivity values. This requires

some basic model assumptions and prior knowledge of the site to narrow the solution space and allow the software to calculate likely models.

Resistivity values are engineering values, themselves, but can be used with local ground truth information, such as bore logs, trenches and construction documentation to determine the underlying material types at a survey site. Resistivity methods are particularly effective at detecting the presence of water or shallow bedrock, since these materials represent very sharp contrasts compared to clays and silts.

1.2 Surface Wave Methods

While resistivity methods characterize the subsurface by its resistance to current, surface waves use stress wave propagation to determine the stiffness of the ground below. The two types of seismic waves, whose motions are shown in Figure 1-5, are body waves, which propagate through the interior of a body, and surface waves, which propagate along a free surface. In geophysical testing, the two primary surface wave types are Rayleigh and Love.

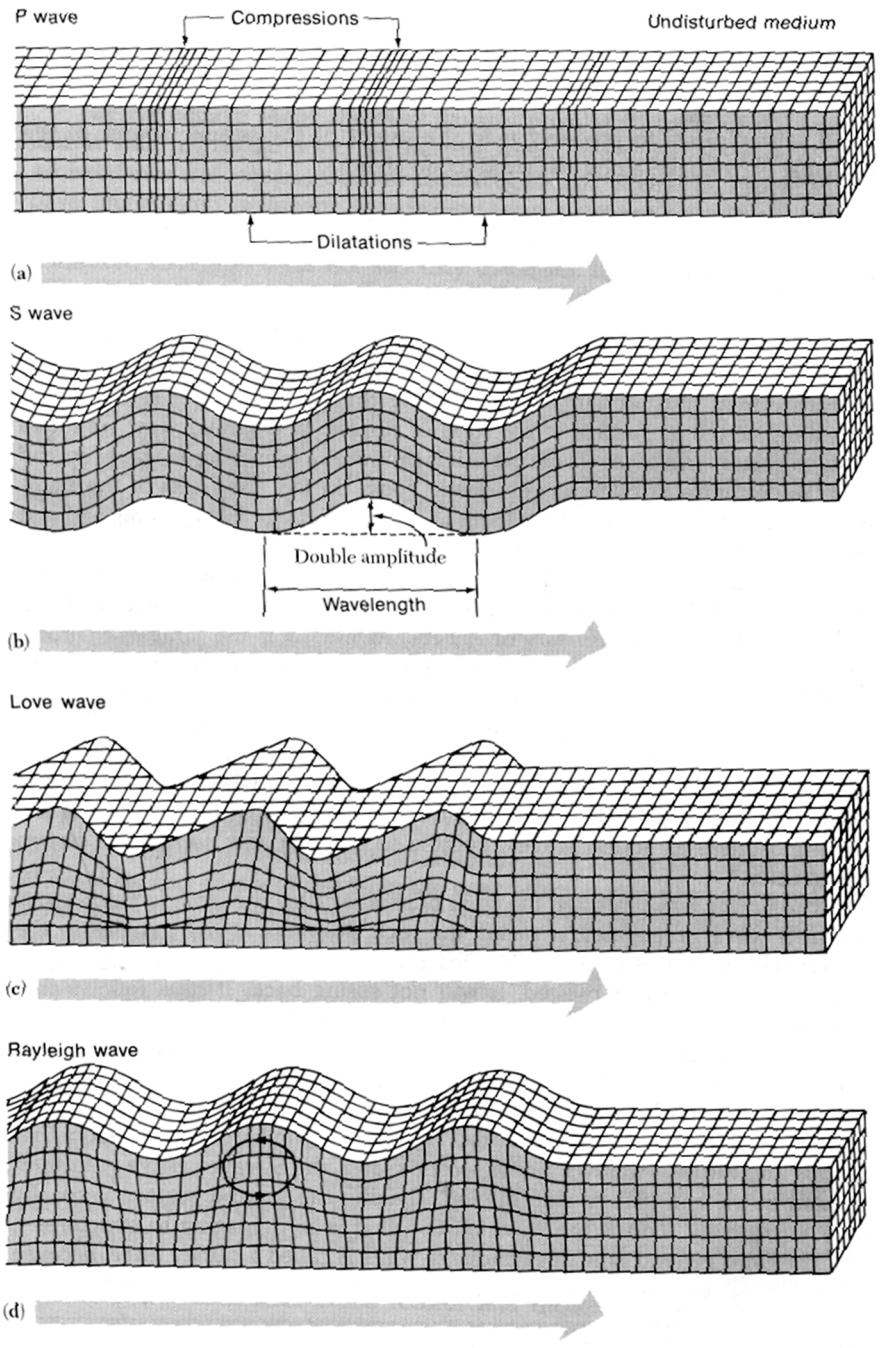

Figure 1-5. Body and surface wave motions: a) p-waves, b) s-waves, c) Love waves, d) Rayleigh waves (Bolt, 1993).

Rayleigh waves were first predicted by their namesake, Lord Rayleigh, in 1885 (Strutt, 1885). In a homogeneous, elastic half-space with no free surface boundary condition, only compression and shear waves (body waves) can be produced. However, with the introduction of

a free surface, non-dispersive Rayleigh waves are formed along that surface with displacements constrained to a depth of 1 – 2 times the wavelength of that wave. While Rayleigh waves are the only surface waves that can exist in a homogeneous half-space, A.E.H. Love predicted in 1911 that heterogeneous half-spaces allow the existence of what became known as Love waves (Love, 1911). Love waves can develop only in a half-space overlain by a layer of less stiff material and consist of horizontally polarized shear waves interacting with wave reflections at that layer boundary, whereas Rayleigh waves form from the interaction of compression and vertically polarized shear waves (Love, 1927) (Ben-Menahem & Singh, 1981).

Surface waves have long been of interest to seismologists for characterization of the interior of the Earth, though it required the development of numerical methods and geotechnical instrumentation before near-surface applications became popular. Van der Poel (1951) performed one of the first documented applications of surface waves using a generator with eccentric weights and oscillograms to calculate dynamic Young's moduli and assess the rigidity of construction layers in roads. The first solutions to the surface wave inversion problems on theoretical dispersion curves came about in the 1950s with advances in computation, but dispersion curve fitting would not be developed until Nazarian and Stokoe (1983) did it manually by trial and error (Thomson, 1950).

The Steady-state Rayleigh method developed by Jones (1962) became the first engineering site characterization method. This simple method consisted of a single receiver in line with a vibrating seismic source that generated waves in ultrasonic frequencies to assess the thickness and elasticity of, at first, concrete slabs and, later, soil columns using lower frequencies. By moving the receiver away from the source with a constant frequency, wavelengths and phase velocities for that frequency could be calculated and by repeating the

process for multiple frequencies, a composite dispersion curve could be obtained. Jones tested soils with both Rayleigh and Love waves and recognized the necessity of changing the source configuration to generate the desired waves, i.e. a vertically vibrating source generates Rayleigh waves and a horizontally vibrating source generates Love waves.

Surface wave methods became much more common with the development of the Spectral Analysis of Surface Waves (SASW) in the 1970s and 1980s (Nazarian & Stokoe II, 1983) (Heisey & Stokoe II, 1982). This two receiver approach, illustrated in Figure 1-6, yields a dispersion curve by estimating travel times for surface waves over a limited frequency range. By varying the receiver spacing, a composite dispersion curve over a larger testing range can be obtained. Despite its long and difficult testing procedure, SASW became much more popular in civil engineering site characterization.

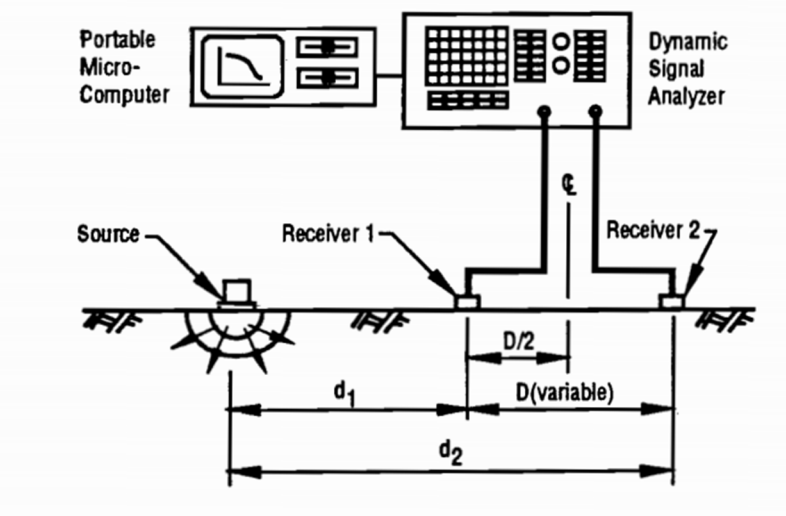

Figure 1-6. SASW testing schematic (Rix, et al., 1991).

In 1987, Gabriels et al. (1987) demonstrated the first application of multichannel surface wave methods, however, until advances in computing and signal processing were made, SASW remained the primary surface wave testing method. In the early 2000s, the Multichannel

Analysis of Surface Waves (MASW) became a robust and effective method for surface wave assessment and resulted in a boom in surface wave applications in civil engineering projects (Park, et al., 1999). MASW generally consists of a seismic source in line with a linear array of receivers, as shown Figure 1-7. The MASW's use of multiple receivers results in faster data collection in the field and more robust data.

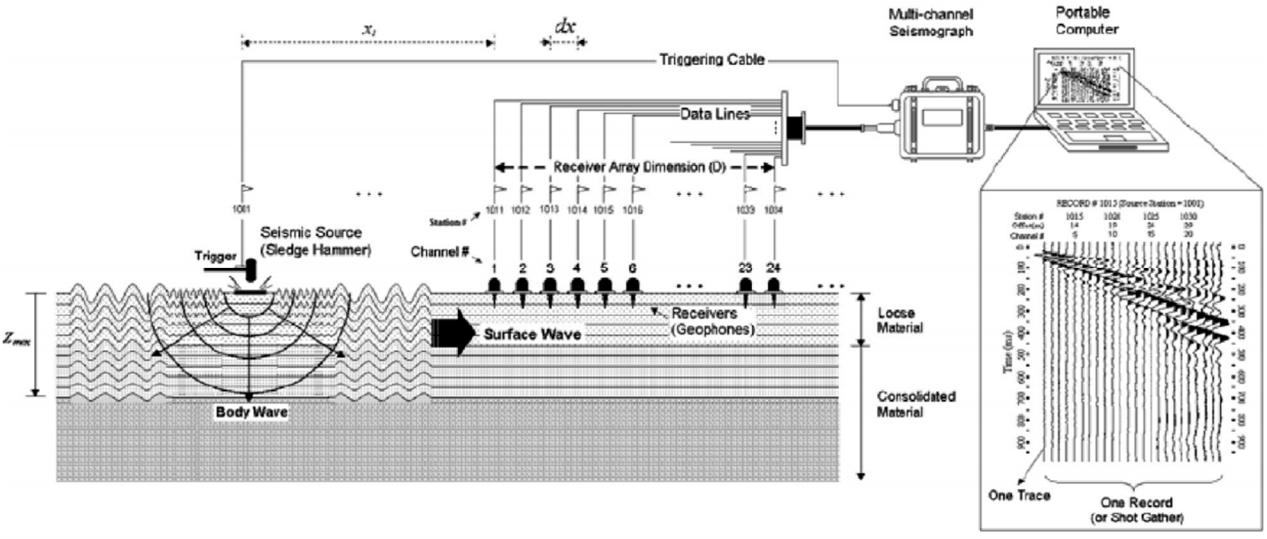

Figure 1-7. MASW schematic showing the wave motion from source to receiver array to signal processing (Mohamed, et al., 2013).

After MASW data collection, several signal processing methods, usually transform based, can used to transform time-space domain data (field data) to another domain where phase velocities for given frequencies can be obtained resulting in a dispersion curve, an example of which is shown in Figure 1-8. Once a dispersion curve is obtained, that curve has to be processed to remove noise, undesired higher modes, and near- and far-field effects. Near-field effects are the result of interference from body waves and the surface wave front. Near the seismic source, the wavefield is a complicated mix of p-waves, s-waves, and surface waves because the various wave types have not yet separated and attenuated. Thus the body waves have an exaggerated influence on the displacements recorded by the receivers within 0.5 – 2 wavelengths of the

source (Foti, et al., 2015). The other source of near-field effects is the shape of the surface wave wavefront. In the various surface wave methods, the expansion of surface waves is assumed to be planar, when it is actually cylindrical requiring the use of cylindrical coordinate beamformers rather than planar, at the cost of increased computing requirements (Zywicki & Rix, 2005). Near-field effects due to body wave interference are lessened in MASW by using relatively long source-offsets and longer arrays, both of which allow wavefronts to separate, attenuate and be identified in processing at the cost of high-frequency dispersion data. Far-field effects result from the wave losing energy with distance from the source and becoming indistinguishable from environmental noise.

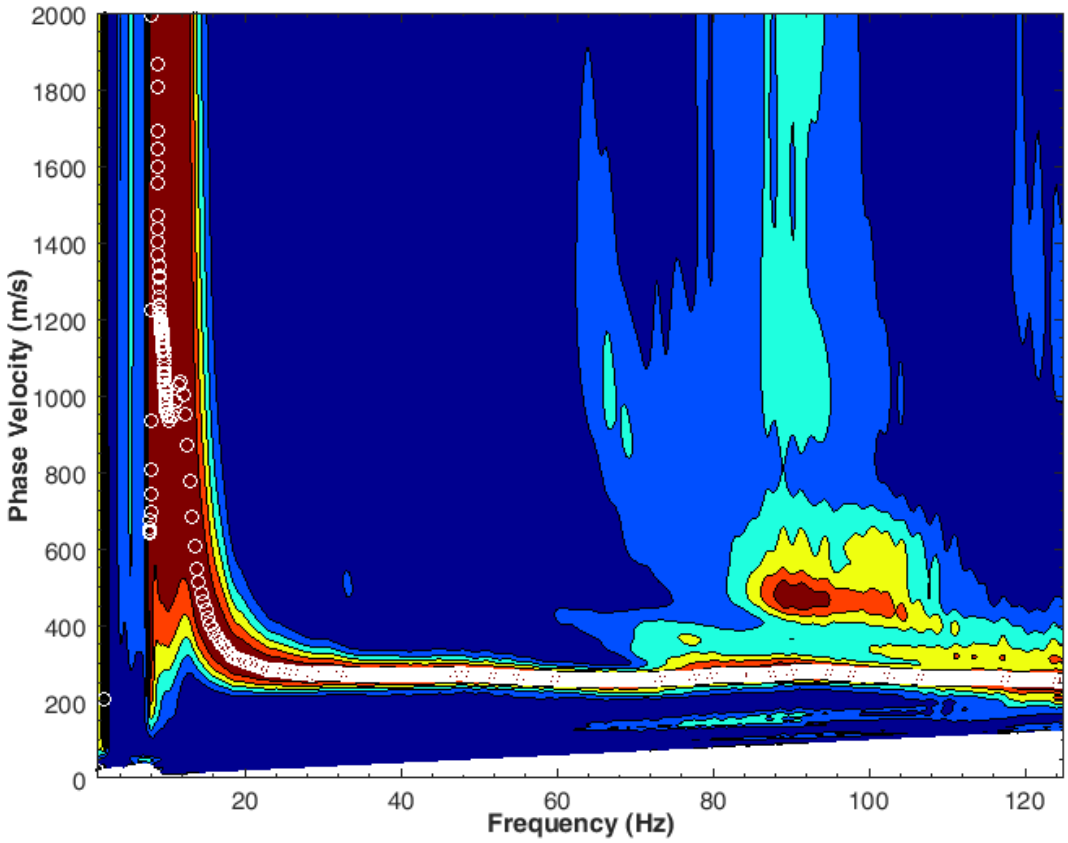

Figure 1-8. Example dispersion curve from Kinion Lake Dam.

Obtaining a subsurface shear wave velocity model requires forward modeling and the solution of an inversion problem, much like in resistivity methods. After higher modes and noise are removed, a variety of software can be used to process this curve and obtain ultimately obtain a shear wave profile. Generally, solving the inversion problem begins with a trial model for the site whose parameters are used to generate theoretical dispersion curves as shown in Figure 1-9. Through successive model iterations, the differences between the experimental and the theoretical are minimized. The most difficult part of MASW is not the data collection or the dispersion processing, but rather the interpretation and inversion. Inversion software using genetic algorithms to generate thousands of shear wave velocity models while keeping and modifying the best fitting models has become increasingly popular (Wathelet, 2008). The downside of this approach is that inversion problems are ill-posed and have an infinite number of solutions resulting in many possible model solutions and the need for large computational resources to generate these thousands of models. By using ground truth information (e.g. layer depths, material types, schematics) or loosely interpreting the dispersion curves, this initial solution space can be reduced yielding faster processing and better results.

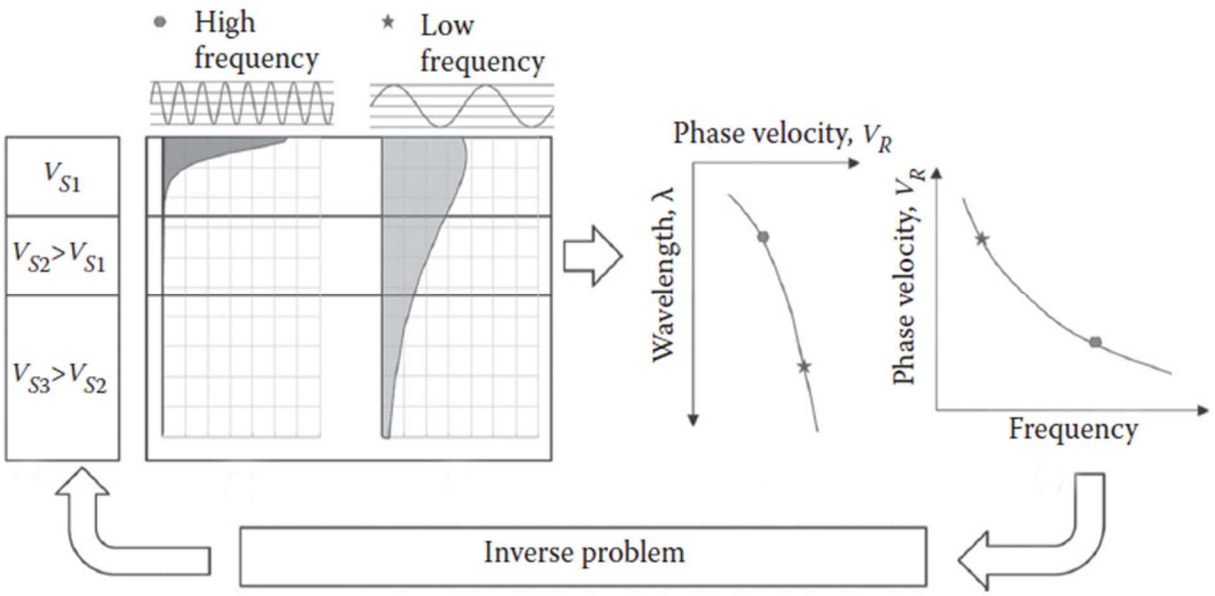

Figure 1-9. General schematic for obtaining a Vs profile solution (modified from Foti et al. (2015)).

Shear wave velocities are a proxy for and can be used to calculate the stiffness of the subsurface materials, allowing the detection of layer boundaries and anomalies. By performing MASW at multiple locations along an earthen structure, a pseudo-2D profile can be constructed, and deviations in shear wave velocities can identify bedrock intrusions, voids, and other features in the subsurface.

1.3 Previous Earth-filled Embankment Dams and Levee Investigations

The United States has an estimated 90,580 dams, the vast majority of which are either rock-fill or earth-fill embankment dams (U.S. Army Corps of Engineers, 2016). Thirty percent of which are considered to have significant or high hazard potential and are in need of repair, resulting in a "D" rating for dams from the ASCE 2017 Infrastructure Report Card (ASCE, 2017). An estimated $45 billion is required to repair the high hazard dams alone, making rapid, economic and accurate assessment of embankment dams integral to national dam safety and maintenance. In a survey of dam failures, Foster et al. (2000) found that overtopping and piping

failures combined resulted in 82% of embankment dam failures prior to 1986. Installation of a spillway reduces overtopping failures; however, piping and erosion through the dam or foundation is still responsible for 44.5% of embankment dam failures to date. The geophysical methods discussed in this thesis have been used before to allow the early detection of internal defects in the nation's dams.

While this thesis specifically focuses on the use of geophysical methods in the assessment of earth-filled dams, both earth-filled dams and earthen levees are similar enough failure modes that previous assessments of levees with methods seldom used on dams can provide valuable insight into the the use of those methods on dams. Both dams and levees can fail by seepage, uplift pressures, piping/internal erosion, sloughing, foundation erosion, and overtopping (U.S. Army Corps of Engineers, 2004; U.S. Army Corps of Engineers, 2000). In fact, the difference between the two types of infrastructure is primarily functional, i.e. "a levee embankment may become saturated for only a short period of time" such as during a flood while dams are constantly retaining water (U.S. Army Corps of Engineers, 2000). The construction of the two types of infrastructure differ primarily in the quality of the materials used in that levees are often built on poor foundations with heterogeneous fill material excavated adjacent to the levee and that earth-filled dams usually have an impervious core or trench to prevent seepage.

Geophysical methods have the potential to meet the needs of rapid, economic and accurate assessment of dams along with the advantage of typically being non-invasive and non-destructive, making them ideal for the evaluation of hydraulic structures. Geophysical methods have been used with success in the past in dam assessment and evaluation with the most common methods measuring resistivity along a dam's crest and toe and measuring shear wave velocities in the same locations using surface wave methods (Cardarelli, et al., 2014; Min & Kim, 2006).

Since soil resistivity is dependent on many parameters including saturation, porosity, temperature, gradation and mineralogy , resistivity methods allow the potential detection of seepage and differentiation between material strata in the dam core and foundation. Surface wave methods, on the other hand, measure shear wave velocities, which can be associated with the stiffness of the materials, allowing detection of potential weathering, different material strata, and internal defects in the dam. Wang et al. (2016) found success using Multichannel Analysis of Surface Waves (MASW) and microtremor array measurement (MAM) methods to determine the internal structure of the Higashi-Takezawa landslide dam. Similarly, Min and Kim (2006) used a 3D surface wave inversion model to assess the internal structure of an earthen dam, though they found that dam geometry could distort the resulting dispersion curves and that source energy and frequency limitations made it difficult to assess dam materials at depths greater than ten meters. Cardarelli et al. (2014) used MASW to characterize the foundation material of an earthen embankment dam, which proved consistent with the other methods they used, including shear wave tomography with about one meter of depth uncertainty. Regions with many embankment dams have seen benefits in resistivity measurements for detecting seepage and erosion, particularly in Sweden. Johansson and Dahlin (1996) used resistivity and temperature measurements in two dams along the Faxälven River to monitor seepage through the dam and its association with seasonal resistivity variations. Sjödahl et al. (2005) performed resistivity surveying along the length of the two Enemossen dams, which resulted in high quality data allowing them to associate known dam problem areas with low resistivity features, even if resistivity alone could not be used to determine those problems. Similarly, Sjödahl et al. (2008) used daily Wenner-Schlumberger Electrical Resistivity Imaging (ERI) measurements along the crest of an earth-filled embankment dam at Hällby to detect internal erosion and seepage from

the lack of fines in the core of the dam while noting that seasonal changes can have significant effects on resistivity values due to temperature and retained water ion content (Total Dissolved Solids). In India, Panthulu et al. (2001) used 2D resistivity profiling along earth-filled dam crests to detect shear and bedding joints in the rock foundations, as well as weathered pockets and seepage paths and recommend performing seasonal monitoring to detect hazardous levels of seepage. More generally, Rein et al. (2004) documented the seasonal and local conditions that affect resistivity measurements most strongly, (e.g. temperature and saturation). Further limitations of resistivity methods are that increased water contents result in lower resistivity values, but that same water presence can indicate seepage and possibly resulting in the transport of fines out of the interior of the dam, yielding in higher resistivity values in future testing. This means that a specific resistivity value does not necessarily indicate a particular material, but can be used along with other site information to interpret the subsurface (Sjödahl et al. (2008)).

Although, the combined use of resistivity and surface wave methods is not extremely common in dam evaluations, it is very common in levee evaluation. Earthen levees have a great deal in common with embankment dams in that the United States levee infrastructure is rated a "D-" in the same 2017 ASCE Infrastructure Report Card (ASCE, 2017). In addition, earthen levees share many of the same failure mechanisms as embankment dams. Levees, however, experience slope failure often than dams, but both have similar geometry and geotechnical materials. Samyn et al. (2014) for example, used Capacitively Coupled Resistivity (CCR) and MASW to identify areas of material weakness corresponding to karst features in French dykes. Similarly, Inazaki and Hayashi (2011) Hayashi and Konishi (2010), and Inazaki and Sakamoto (2005) tested levees at 20 locations in Japan, identifying features like paleo-channels and pipes with CCR and MASW methods.

To our best understanding, full waveform inversion (FWI) approach has not been reported for evaluation of dams or levees, and thus its capability for this application merits investigation. As reviewed by Vireux and Operto (2009), by extracting information contained in the complete waveforms, the FWI approach offers the potential to produce higher resolution models of the subsurface than approaches that consider only the dispersive characteristic of Rayleigh waves or first-arrival times of body waves. The FWI approach has been used widely to characterize subsurface structures at kilometer scales. However, at geotechnical scales (< 30 m in depth), inherent issues include inconsistent wave excitation, strong attenuation, strong variability of near surface soil/rock lithology, and poor a priori information. These issues tend to produce significant inversion artifacts particularly at shallow depths. The artifacts likely produce local solutions and limit depths of investigation, and thus prevent FWI methods from being used for geotechnical site characterization on regular basis. An advanced Gauss-Newton FWI method (Tran and McVay, 2012; Tran et al, 2013; and Tran and Luke, 2017) has been developed as an effort to reduce shallow artifacts for better resolving deeper structures. Its capability for dam characterization is investigated in this study by using the same dataset collected for the MASW method, and the FWI result is compared to MASW results and drillings for verification.

Even though there are a number of examples of resistivity methods and surface wave methods being used to evaluate earthen dams, very few studies have directly compared the results from different resistivity methods, surface wave methods utilizing different surface wave types (Rayleigh and Love) and full waveform inversion (FWI) methods. This paper details the geophysical evaluation of Kinion Lake Dam using a combination of geophysical methods including ERI, CCR, MASW, and FWI. The history of the dam and the surrounding geology of the site is first explained. This is followed by an explanation of the geophysical methods used in

the study, survey parameters for the dam and a discussion of data processing. Finally, the results are presented and interpreted along the centerline crest of Kinion Lake Dam and the downstream toe. The effectiveness of each method at identifying the subsurface layering of the dam and providing insight into the potential problem areas of the dam are discussed.

This thesis details the geophysical evaluation of Kinion Lake Dam using multiple resistivity and surface wave methods. The history of the dam and the surrounding geology of the site is first explained. This is followed by an explanation of the geophysical methods used in the study, survey parameters for the dam and a discussion of data processing. Finally, the results are presented and interpreted along the centerline crest of Kinion Lake Dam and the downstream toe. The effectiveness of each method at identifying the subsurface layering of the dam and providing insight into the potential problem areas of the dam are discussed.

1.4 Site Background

Kinion Lake Dam is a 342 meter long and 15 meter tall earthen dam located in Washington County, Arkansas, shown in Figure 1-10. The local geology consists of an eroded plateau overlaying shales and sandstones with valleys cut into cherty limestone. Nearby bedrock outcrops consist of very weathered limestone punctuated with fissures, joints, and caverns. This cherty limestone layer has an average thickness of 7 – 9 meters and the cherty gravel is typically filled with fines (NRCS, 2011).

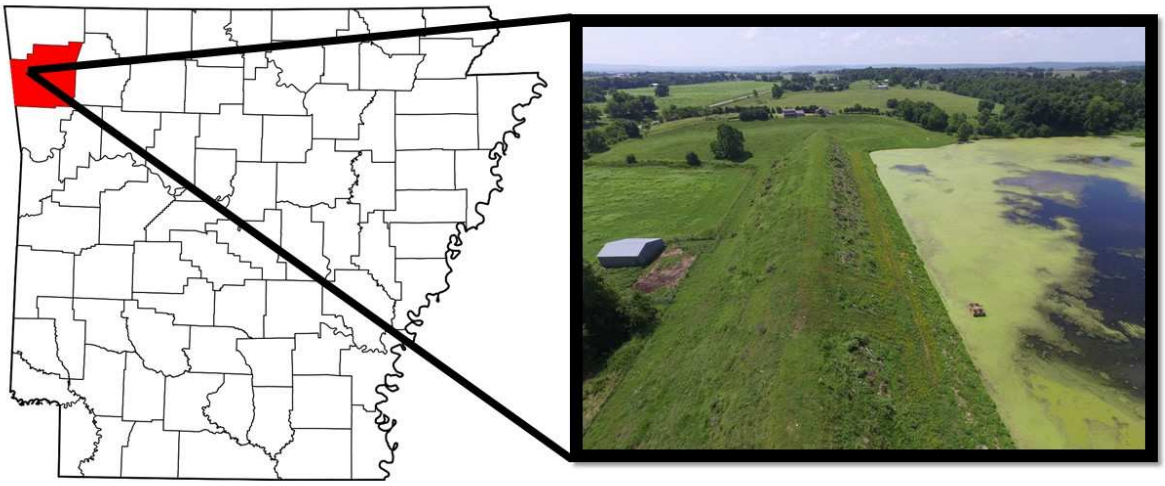

Figure 1-10. Location of Kinion Lake Dam in Washington County, Arkansas.

The dam was initially constructed in 1964 and immediately began experiencing seepage issues due to the local geology (NRCS, 2011). Prior to a 1969 drilling and grouting project, the structural integrity of the dam came under scrutiny as large sinkholes began forming, allowing large quantities of water to pass either through the dam, under the dam or through the abutments. This flow had the additional drawback of removing substantial quantities of fines from the interior of the dam and/or its foundation material (SCS, 1970). In 1969, Kinion Lake Dam was drilled and grouted in several locations along its length; however, it was unclear whether the grouting was successful because Kinion Lake experienced a severe drawdown due to a drought. Following the drought, seeps continued to form and in 1984, a foundation treatment consisting of backfilling the solution channels with high-plasticity clay and silt was performed and a foundation drain was installed (SCS, 1970). Even after these additional treatments, large seep areas continued to be documented, including a 20 feet wide seep that had broken the sod and jetted water six inches into the air. These seeps were in the same locations as those previously documented in the 1969 drilling report and the 1982 field inspection (NRCS, 2011). Additionally, the 1969 drilling explorations also located springs at the junction of the toe of the

dam and the left abutment, seeps on the slope of the embankment, and a large spring with an estimated flow of 7500 liters per minute downstream (SCS, 1970).

Conclusions from the SCS (SCS, 1970), describe the bedrock under the dam as limestone with significant chert content and a general low resistance to weathering and ground water action. Solution cavities, infill of fines, and fractures made distinguishing between the bedrock and the gravelly soil overburden very difficult and somewhat ambiguous during drilling. This weathered bedrock foundation material allows almost unimpeded flow both through the dam and laterally, along cracks in the upper portion of the foundation. The bedrock profile under the dam, determined during the original 1963 evaluation, is shown in Figure 1-11. The contour of the bedrock was found to be mostly level until inclining near the spillway, though some shallower regions were located at the 60, 140 and 180 m marks.

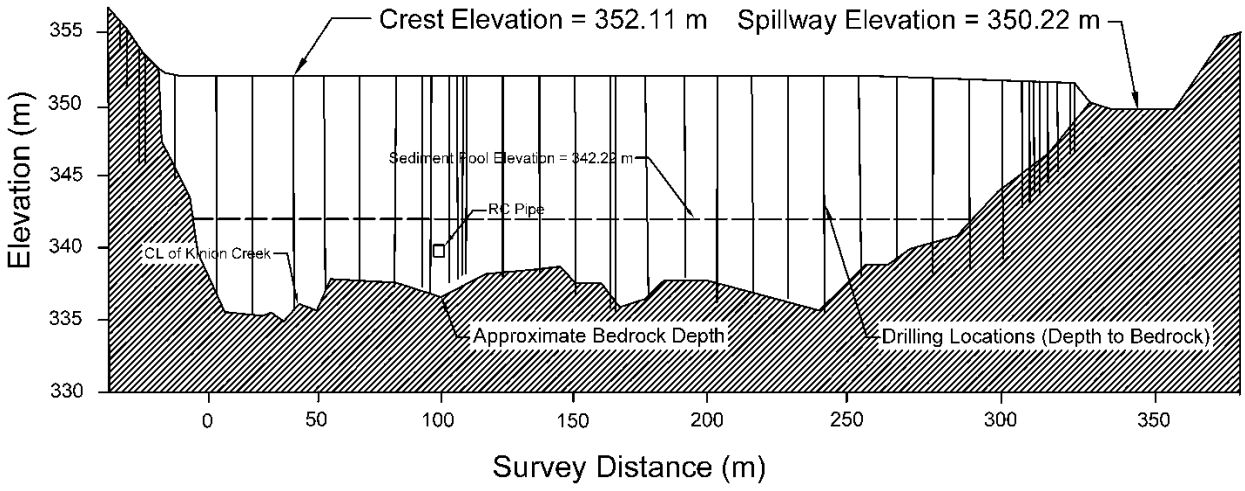

Figure 1-11. Bedrock profile modified from the 1963 drilling and grouting report showing depths to bedrock encountered during drilling (SCS, 1970).

2 Geophysical Investigation

The geophysical investigation of Kinion Lake Dam was conducted using a combination of geophysical methods including ERI, CCR, MASW, and FWI. The data were collected using

each method over the period of approximately one year from July 2015 to March 2016. Data was collected along the centerline crest of the dam and along the downstream toe where seepage had been observed. The testing location along with testing parameters and data processing parameters are detailed for each method below.

Electrical resistivity is a quantification of how strongly a given material opposes the flow of electrical current. The electrical resistivity of earth materials can vary depending on the porosity, texture, degree of saturation, chemical makeup of the pore water, temperature, and clay content of the material (Kaufman & Hoekstra, 2001). However, in general resistivity values range from 10-20 Ohm-m for water, up to 75 Ohm-m for clays, from 26 – 240 Ohm-m for silts, 96-450 Ohm-m for sands and anything more resistive likely indicates an absence of water or an abundance of hard, resistive materials like gravels and rock (Kaufman & Hoekstra, 2001). As shown by these ranges, there is significant overlap between the different materials primarily depending on the degree of saturation of the material (Mofarraj, 2017).

Resistivity measurements are made in the field by inducing a current into the ground at one location and measuring the change in potential at another location. Traditional direct current ERI surveys are conducted using multiple stainless steel electrodes installed in the ground at a uniform spacing along a linear line for 2D surveys. Measurements are taken by inducing a current through an electrode with a direct current and taking electrical potential (voltage) measurements at other electrodes in the array in various sequences (Wenner, Schlumberger, and dipole-dipole). The injection of current and measurement of voltage using multiple pairs of electrodes provides multiple readings of the apparent resistivity of materials at different depths. Through an inversion process, the apparent resistivities and the array geometries can be used to generate a profile matching true resistivity with depths. CCR systems, on the other hand, are

designed to be pulled along the ground rather than utilizing staked electrodes. The method works by inducing an alternating current via capacitive-coupling in the earth by a transmitting dipole and then measuring the potential using a receiving dipole. The measured voltage will be proportional to the resistivity of the earth between the two diploes and the current delivered by the transmitting dipole. The transmitter and receiver can only be setup in a dipole-dipole configuration for surveys. The apparent measurement depth is determined by the dipole length and the distance between the receiver and the transmitter. Testing at several sites has shown that the CCR response is nearly identical (within 2%) to that of a dipole-dipole DC resistivity measurement (Pellerin, et al., 2003). However, other work has shown differences between the two methods thought to be the result of violating assumptions (required low induction number, non-point source, and effective dipole lengths) of the CCR theory (McNeill, 1980; Oldenborger, et al., 2013; Sapia, et al., 2017). However, often one of the limitations of the CCR method (especially for dam investigations) is the limited investigation depth of CCR (typically 6-15 m versus 20 to >40 m depth for ERI) (Asch, et al., 2008) but CCR typically provides better near surface resolution compared to ERI (Garman & Purcell, 2004).

Surface wave methods utilize the dispersive properties of surface waves (Rayleigh or Love) to determine the small strain shear wave velocity structure of the subsurface (Park, et al., 1999). Rayleigh waves have traditionally been the wave of choice for surface wave methods because Rayleigh waves are simpler to generate and sample in the field. However, Love wave use has increased significantly in the past decade. Love waves have been shown to provide more coherent data at difficult sites (i.e., shallow bedrock sites) and provide additional constraint to the inversion problem (Wood et al. 2014). Surface wave methods can broadly be split into two categories: (1) active source methods and (2) passive source methods. Active source methods are

more commonly used for near surface site characterization whereas passive source methods are generally used for deep site characterization. Active source methods generally use a linear array of sensors to measure the phase velocity of waves emanating from a known source (typically located in-line with the array) and propagating past the receivers. By measuring the phase angles between sensors for a range of surface wave frequencies, an experimental dispersion curve is developed which relates surface wave velocity to frequency or wavelength. An inversion process is then used to develop the shear wave velocity (Vs) profile at the site. This inversion process uses a numerical solution, which propagates Rayleigh or Love type surface waves over a layered half-space with each layer being assigned properties such as shear wave velocity, thickness, unit weight, and compression wave velocity. The numerical model solves for the theoretical dispersion of surface waves over this layered half-space. The theoretical dispersion curve is then compared to the experimental dispersion curve. Model parameters are updated until the theoretical dispersion curve matches the experimental dispersion curve for the site.

The MASW method (Park, et al., 1999) is an active source surface wave method that uses a linear array of typically 24-48 receivers to measure surface wave phase velocities in the field. Typically, a constant spacing between receivers is used along with a sledgehammer source to generate surface waves. Through a two dimensional transform such as the frequency-wavenumber transform, an experimental dispersion curve is developed. Several other dispersion analysis techniques exist (f-k, f-p, Park transform, beamformer) to process the raw signals recorded in the field. Despite the method used to generate the experimental dispersion curve, a fundamental or fundamental and higher mode inversion analysis is often used to match the experimental data and obtain a Vs profile. The Vs profile for the array is a function of the material over the lateral extent of the array. However, the 1D Vs profile generated from each

analysis is considered to be more representative of the material located at the center of the array. To understand lateral variations in Vs using the MASW method, multiple tests are conducted by moving the receiver array forward or backward along a line and repeating the test. The multiple 1D Vs profiles are then stitched together along the survey line to create a pseudo 2D profile that describes the variation of Vs with depth and distance along the line. These pseudo 2D profiles can be particularly useful for mapping subsurface layers at a site. Typical shear wave velocity ranges include soft soils in the <180 m/s range, stiff soils between 180 and 360 m/s, highly weathered rock and dense soil between 360 and 760 m/s and weathered to fresh rock at anything greater than 760 m/s.

2.1 Electrical Resistivity Imaging (ERI)

ERI surveys were performed from June 15-22, 2015, along the centerline crest and the downstream toe of Kinion Lake Dam using an AGI SuperSting R8/IP system. GPS locations for the electrode data were recorded and are shown in Figure 2-1. The dam crest survey consisted of a linear array of 112 electrodes at a 1.22 m spacing, while a 0.6 m spacing was used on the downstream toe. To profile the entire dam while maintaining the higher resolution of close electrode spacing, a ¼ array (30 probes or 36 m) roll along was conducted following each test setup. Testing was conducted using the Schlumberger and dipole-dipole configurations. The apparent resistivity data collected in the field was inverted using AGI EarthImager 2D CRP software. ERI data was collected and processed by the Natural Resources Conservation Service (NRCS, 2016).

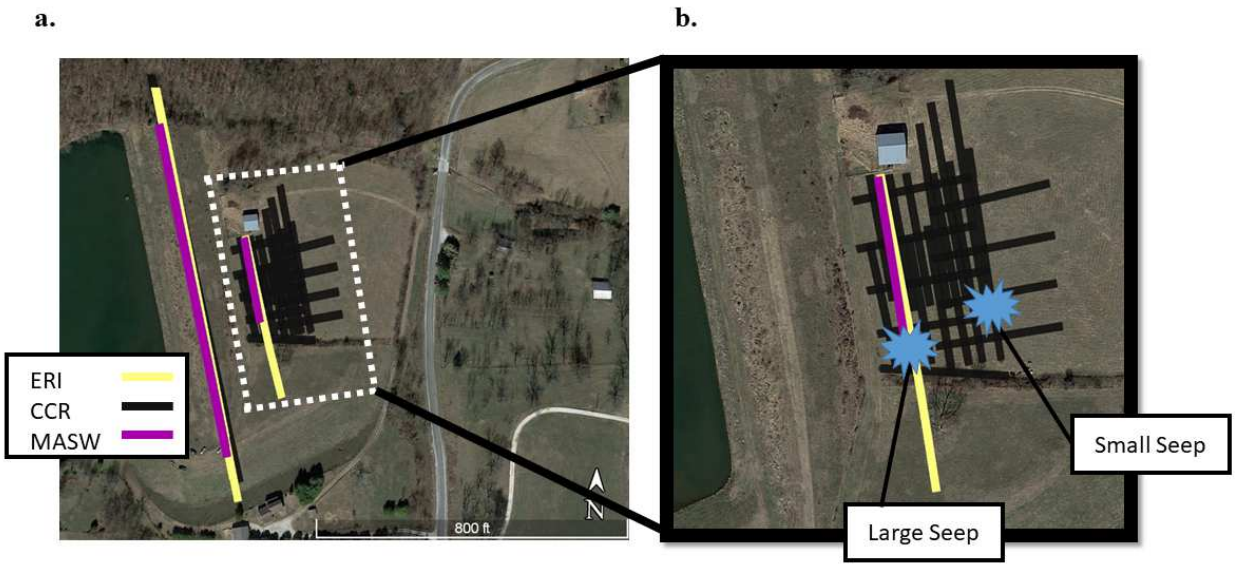

Figure 2-1. Survey locations for at Kinion Lake Dam lines a) Survey locations along the centerline crest of the dam and b) grid survey along the downstream toe (location of previous seepage is shown) (from Google Maps).

2.2 Capacitively Coupled Resistivity (CCR)

CCR surveys were performed on March 16, 2016 by University of Arkansas personnel, along the centerline crest of the dam using a Geometrics OhmMapper TR5 system (see Figure 2-2) which utilizes five receivers to detect current injected into the ground via a transmitter at the end of the array. The location of the operator was continuously recorded using a Trimble Geo7x GPS unit. To provide comprehensive measurements of the entire dam, dipole lengths of 5 meters and 10 meters in combination with rope lengths of 5 meter, 20 meter, 25 meter and 40 meter were utilized during testing. Short dipole lengths in combination with short rope lengths measure very near surface materials while longer dipole lengths and longer ropes lengths measure deeper materials. A gridded survey was also performed along the downstream toe of the dam (Figure 2-1b), overlapping with the previously performed ERI survey. A single diploe length of 5 meters along with a rope length of 5 meters was utilized during testing.

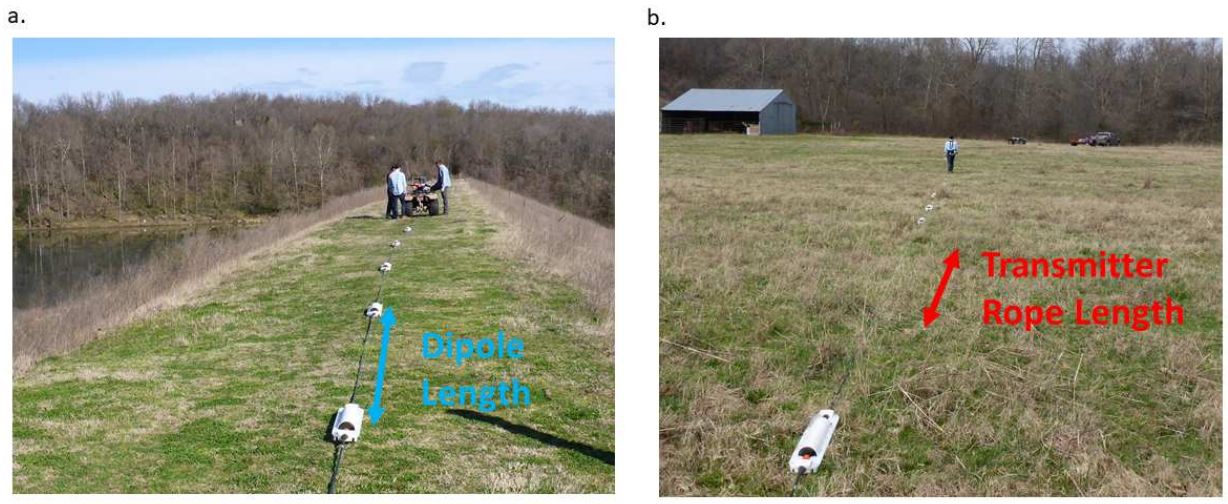

Figure 2-2. OhmMapper arrays: a) linear surveys pulled by ATV b) grid survey pulled by harness.

The raw OhmMapper data was first processed in Geometrics OhmImager to correct any metadata (rope-length, dipole length, operator offset) errors and to combine resistivity data for common locations before being exported to MagMap (Loke & Barker, 1996). MagMap was used to convert GPS data to UTM, remove dropouts and spikes from the apparent resistivity data, and export profile data for use in Res2dinv (Loke & Barker, 1996). Res2dinv uses a smoothness-constrained least-squares method incorporating damping factors to obtain an inversion solution (Loke & Barker, 1996). A 1.25 m cell size and large dataset optimization options (optimized Jacobian, fast, approximate Jacobian matrix calculation, and a sparse inversion) were utilized during the inversion.

2.3 Multichannel Analysis of Surface Waves (MASW)

MASW using Love and Rayleigh type surface waves, hereafter referred to as $MASW_L$ and $MASW_R$, respectively, was performed along the crest of the dam and along the downstream toe on September 10th, and 15th, 2015, respectively. Testing was conducted by the University of Arkansas with testing locations shown in Figure 2-1. Surface waves were measured using a

linear array of 48, 4.5 Hz vertical and horizontal geophones with a 1 m uniform spacing between geophones (a total array length of 47 m). The geophones were attached to a landstreamer system allowing them to be dragged rather than staked, increasing the rate of testing. A sledgehammer source was used to generate Rayleigh waves (vertical hits, Figure 2-3a) and Love waves (horizontal hits, Figure 2-3b). For both tests, source positions of 10 m and 1 m from the first and last geophone, as well as at the quarter, half and three quarter points were utilized at each array location (i.e., a total of seven source positions for each array location). At each source position three sledgehammer blows were stacked to improve the signal-to-noise ratio of the data. After each setup, the array of receivers was pulled forward 24 m, so that the first receiver would be located where the 24th receiver was located for the previous array (i.e., a 1/2 roll-a-along) resulting in ten setups total for the crest of the dam, and two setups along the downstream toe.

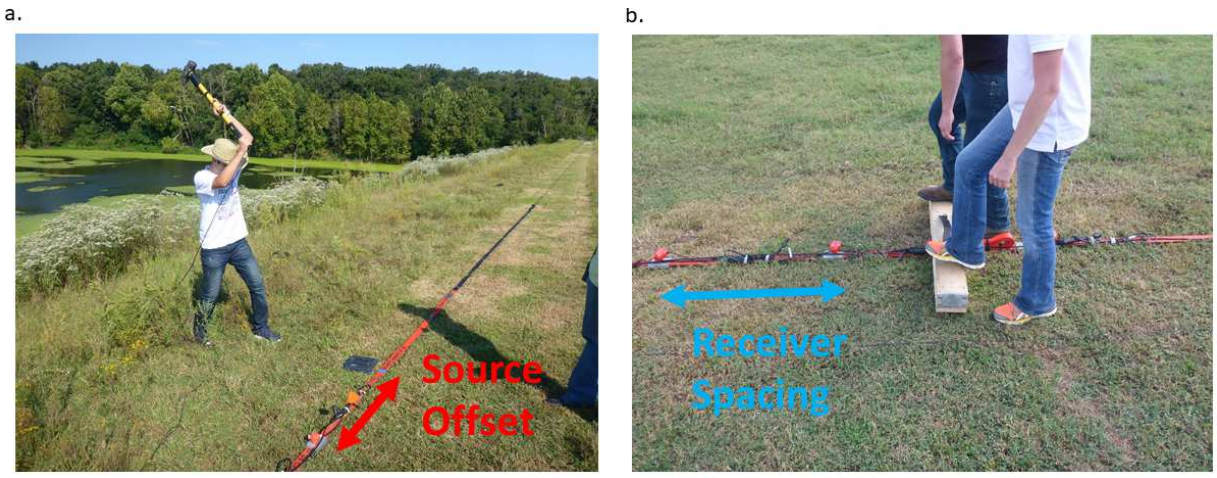

Figure 2-3. a) A strike plate is used for Rayleigh wave acquisition. b) A strike beam is used for Love wave acquisition.

The experimental MASW data was processed using the frequency domain beamformer method in Matlab (Zywicki & Rix, 1999). Each 48 channel array was subdivided into 24, 24 channel arrays with a separation of one geophone spacing between arrays (e.g. channels 1 – 24, 2 – 25, 3 – 26, etc), allowing for a dispersion curve to be obtained for every 1 m of the array, while

reducing the number of source positions needed for testing. Offsets appropriate for MASW, (e.g. channels 1 – 24 include source locations of -10, -1, 36.5, 48, and 57 m) were used for each subset of channels. Multiple source offsets are used as a means to: (1) identify potential near-field effects, (2) aid in selecting the fundamental mode of surface wave propagation, and (3) provide a robust means for estimating dispersion uncertainty (Cox & Wood, 2011). The maximum spectral peak in the frequency-wavenumber domain was picked automatically for each frequency to reduce user bias. Dispersion points clearly displaying near field effects, effective modes, or obvious inconsistencies were removed from the data. However, much of the "normal" dispersion scatter was left intact to estimate uncertainty. The composite dispersion curve was developed using all source offsets for a particular 24 channel subset. The data were divided into 50 frequency bins from 1-100 Hz using a log distribution. The mean and standard deviation were estimated for each data bin resulting in a mean experimental dispersion curve with an associated standard deviation. This mean dispersion curve was then inverted using the software package Geopsy (Wathelet, 2008). Multiple parameterization options (i.e., variations in the number of layers and potential thickness of those layers) were attempted for the datasets. The best parameterization was found to consist of 10 layers with each layer thickness allowed to range from 0-3 m. The shear wave velocities of the layers were allowed to vary from 150 m/s to 3500 m/s. For each dispersion curve, 200000 Vs models were generated using the neighborhood algorithm in Geopsy. The goodness of fit was judged based on the misfit parameter (collective squared error between experimental and theoretical curves) and using visual inspection. The median of the 1000 best (lowest misfit) Vs profiles was taken as the 1D Vs profile for each sub-array. The individual 1D Vs profiles were combined together to develop Pseudo 2D plots of the variation of shear wave velocity with distance along the line and depth.

2.4 Full-Waveform Inversion

The same seismic dataset collected for the $MASW_R$ was analyzed by the FWI method (Tran and McVay, 2012; Tran et al, 2013; and Tran and Luke, 2017). The method is based on a finite-difference solution of 2-D elastic wave equations to generate synthetic waveform data, and Gauss-Newton inversion technique to update material properties (Vs and Vp) until the difference between synthetic and field measured data is negligible. The $MASW_R$ dataset was recorded for 70 shots (10 landstreamer setups and 7 shots each setup), and 68 of them were used for the waveform analysis. The first and last shots (no receivers within 10 m from the shots) were removed, because the FWI method requires a dense source-receiver configuration. The total analyzed distance is 265 m along the dam.

To avoid incorrect local solutions, an appropriate initial model was developed with a consult of the spectral analysis of the measured data, as well as waveform analysis was done in sequence of increasing frequencies (starting with low frequency data requires a less detailed initial model). The 1-D initial model was established with Vs of 300 m/s on the surface and linearly increased to 900 m/s at 24 m depth, for the entire domain of 265 m length (no lateral variation). The depth of 24 m was taken as about a half of the landstreamer length (47 m). The Vp initial model was generated from the Vs profile and a Poisson's ratio of 0.3. Two inversion runs were performed with central frequencies of 15 and 25 Hz, with the lower frequency run first. The bandwidth for each central frequency was 30 Hz with 15 Hz on each side. For example, with the central frequency of 25 Hz, measured signals from 10 to 40 Hz were considered, but signals lower than 10 Hz or higher than 40 Hz were removed by low- and high-pass filtering.

For inversion, the 24 m depth × 265 m length domain was divided into 6360 cells of 1.0 m × 1.0 m. The cell size of 1 m was selected the same as the geophone spacing. Vs and Vp of cells

were updated simultaneously during inversion. The mass density throughout the domain was kept constant at 1800 kg/m^3. Analyses at 15 Hz and 25 Hz were both stopped after 20 iterations, when the change of least-squares error from one iteration to the next is small (less than 1%). It was found that Vs and Vp inverted results are very consistent, and only Vs profile is included in this paper for comparison with those from MASW methods.

3 Results and Discussion

Based on the 1969 drilling report, Kinion Lake Dam consists of three distinct layers: 10 – 12 meters of soft soil, 1 – 5 meters of cherty gravel and cobbles and at 13 – 15 meters below the surface, a fractured limestone bedrock layer (NRCS, 2011). This layering is used as a rough ground truth to estimate the accuracy of each of the geophysical methods at identifying the depth of bedrock across the dam and also at identifying any unique features along the cross section. In addition, intra- and inter- method comparisons will be discussed to understand the variability between the results of each method. The implications of the results will be discussed in regards to their impact on Kinion Lake Dam and on the use of the methods for dam evaluations in general.

3.1 Crest of Dam

The 2D results of the surface wave and resistivity surveys are shown in Figure 3-1 with the drilling report bedrock line overlain. Figure 3-1a and Figure 3-1b represent the raw pseudo 2D dispersion curves for $MASW_R$ and $MASW_L$, Figure 3-1c and Figure 3-1d represent the pseudo 2D Vs results developed from data in Figure 3-1a and Figure 3-1b, respectively, Figure 3-1e represents the full waveform inversion Vs results, and Figure 3-1f and Figure 3-1g represent the CCR and ERI results, respectively. First examining the dispersion plots for $MASW_R$ and $MASW_L$ in Figure 3-1a and Figure 3-1b, which are plotted in terms of pseudo depth (i.e.,

experimental wavelength divided by 2, which approximates depth), reveals a generalized three layer system similar to that described in the NRCS drilling report. Comparing the two plots, a strong velocity increase is observed in the Love wave dispersion data 1-2 meters below the bedrock depth estimated using the 1969 drilling report. A similar velocity increase is observed in the Rayleigh wave dispersion data at a slightly higher depth than observed for the Love wave data. This difference is likely caused by the differences in the dispersion properties of Rayleigh versus Love waves (i.e., wavelength/2 is only a rough estimate of depth and the dispersion properties of the waves are different). Although these plots can be used independently in the assessment of variability across the dam, the true layer thickness and shear wave velocities must be obtained from an inversion process. The primary use of these plots were to develop the inversion parameterization for the site by providing general estimates of initial depths and shear wave velocities of the subsurface.

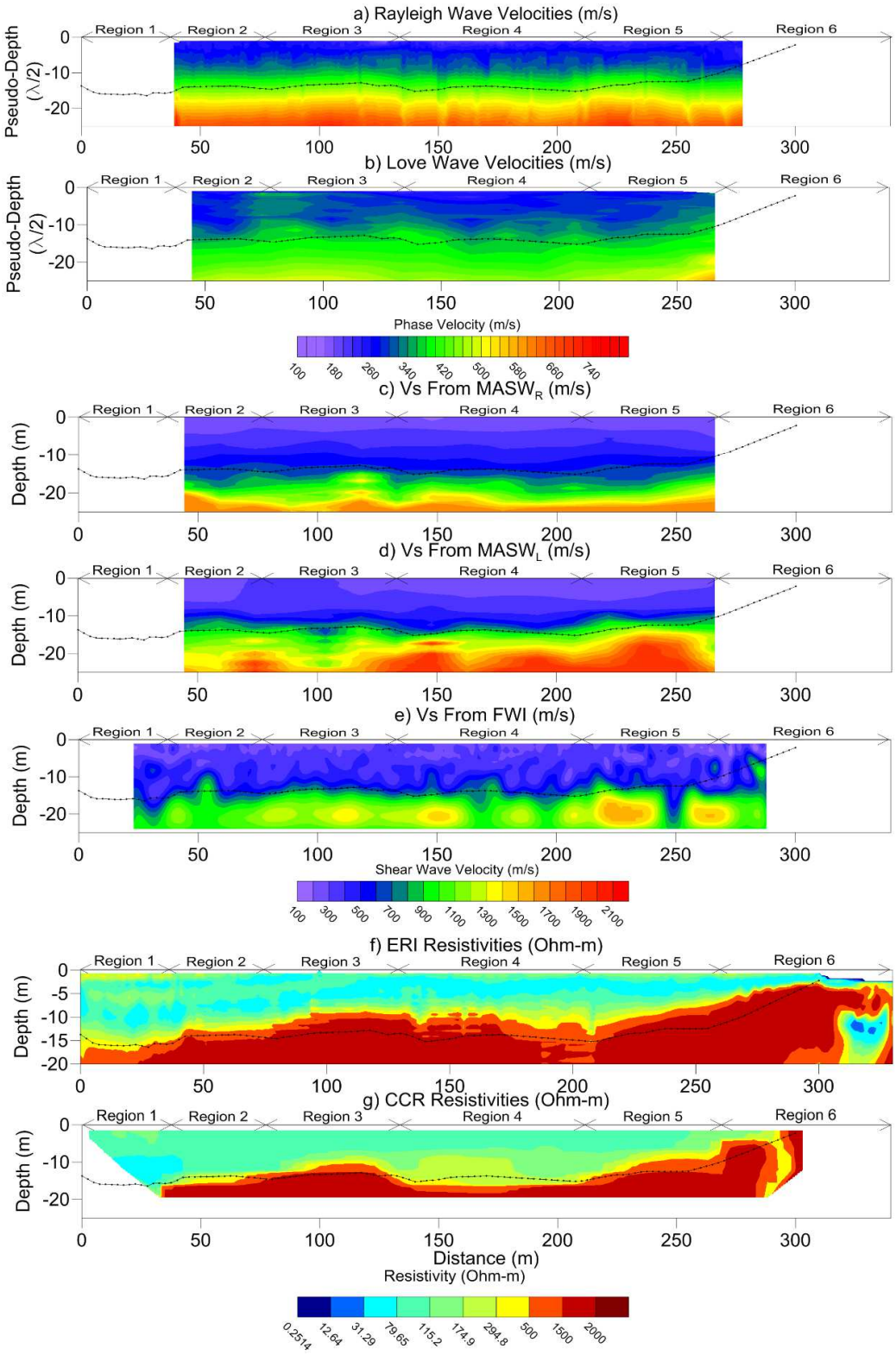

Figure 3-1. 2D Profiles for the crest of Kinion Lake Dam: a) Rayleigh wave dispersion velocities, b) Love wave dispersion velocities, c) MASW$_R$ Vs, d) MASW$_L$ Vs , e) FWI Vs, f)

ERI resistivities, and g) CCR resistivities. The dashed line represents the bedrock line determined from the drilling and grouting report. The labeled regions are areas of interest discussed in the text.

Comparing the three 2D Vs profiles in Figure 3-1c-15e for the $MASW_R$, $MASW_L$, and FWI, respectively, a 10 – 11 meter top layer, a 1.5 – 5 meter transition layer and a stiffer bedrock layer at variable depths (11-14 meters) below the surface can be observed in each plot, with shear wave velocities corresponding to a stiff soil, soft rock, and rock, respectively (ASCE, 2013). This resulting system agrees fairly well with the drilling report; however, the $MASW_R$ Vs results indicate a bedrock depth approximately one meter deeper and the $MASW_L$ Vs results indicate a bedrock depth approximately one meter shallower than the drilling report. In addition, the $MASW_R$ Vs results indicate a thicker weathered rock layer than observed in the $MASW_L$ results. These differences are likely caused by the difference in the experimental dispersion curves generated from each wave type. As shown in Figure 3-2, where typical Love and Rayleigh dispersion images for the dam crest are shown, the Love wave dispersion images (Figure 3-2a) has a significant mode jump from 15-23 Hz while the Rayleigh dispersion images (Figure 3-2b) were mostly continuous throughout. This frequency range corresponds to a depth of 10-15 meters below the top of the dam and is critical to resolving the bedrock depth below the dam. Therefore, having poor data in this region results in more uncertainty in the $MASW_L$ Vs information generated in that region. The FWI Vs results match the bedrock depth from the drilling report best (less than 1 meter difference at most locations), but it results in a much more variable contour (i.e., sharp increases and decreases in bedrock depth). The MASW results indicate more subdued and consistent bedrock depth below the dam. The fluctuation of Vs values from MASW is muted (less extreme) because the results represent averaging over large volumes, whereas Vs values from the FWI are quite localized (cells). These FWI undulations could be real features under the dam or noise artifacts; however, without additional information is it difficult

to confirm either. The FWI may provide a higher resolution image, identifying mores subsurface features than using the MASW profiles.

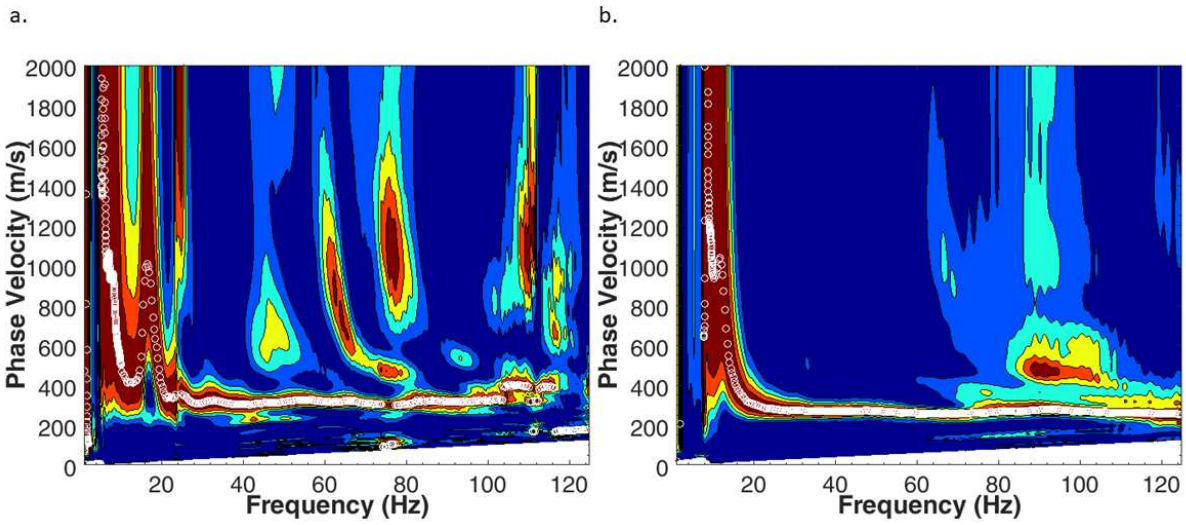

Figure 3-2. Typical a) Love wave and b) Rayleigh wave dispersion images for the crest of Kinion Lake Dam.

Comparing the results from the Vs methods in more detail, the percent differences between the 2D Vs profiles developed using each surface wave method are shown in Figure 3-3. For Figure 3-3a, the percent difference between the $MASW_R$ and $MASW_L$ Vs is shown. For the top 10-12 meters of the cross section (i.e., the stiff soil), the two methods are generally within 5 - 10%, with the $MASW_R$ Vs generally greater than the $MASW_L$ Vs. However, in the weathered rock and rock layers below 10 meters, the differences become greater with typically $MASW_L$ Vs being 25 - 50% greater than $MASW_R$ Vs. This highlights one of the limitation of surface wave methods in that resolving the velocity of the half space in the model (i.e., bedrock in this case) is often difficult due to the lack of long wavelength information (Wood et al. 2014). The percent difference between the $MASW_R$ Vs & $MASW_L$ Vs results and the FWI Vs results are shown in Figure 3-3b and Figure 3-3c, respectively. Comparing the $MASW_R$ Vs and FWI Vs results, the values are typically within 10 – 20% of one another with larger variations (up to +/- 40%)

occurring in somewhat randomly distributed locations. Comparing the $MASW_L$ Vs and FWI Vs results, the $MASW_L$ Vs is 0 – 25% higher than the FWI beyond 20 meters in depth, and generally 0 – 25% lower in the top 10 meters. The difference between $MASW_L$ Vs and FWI Vs are similar to those observed between the two MASW approaches, which makes sense given the FWI and $MASW_R$ were derived from the same dataset.

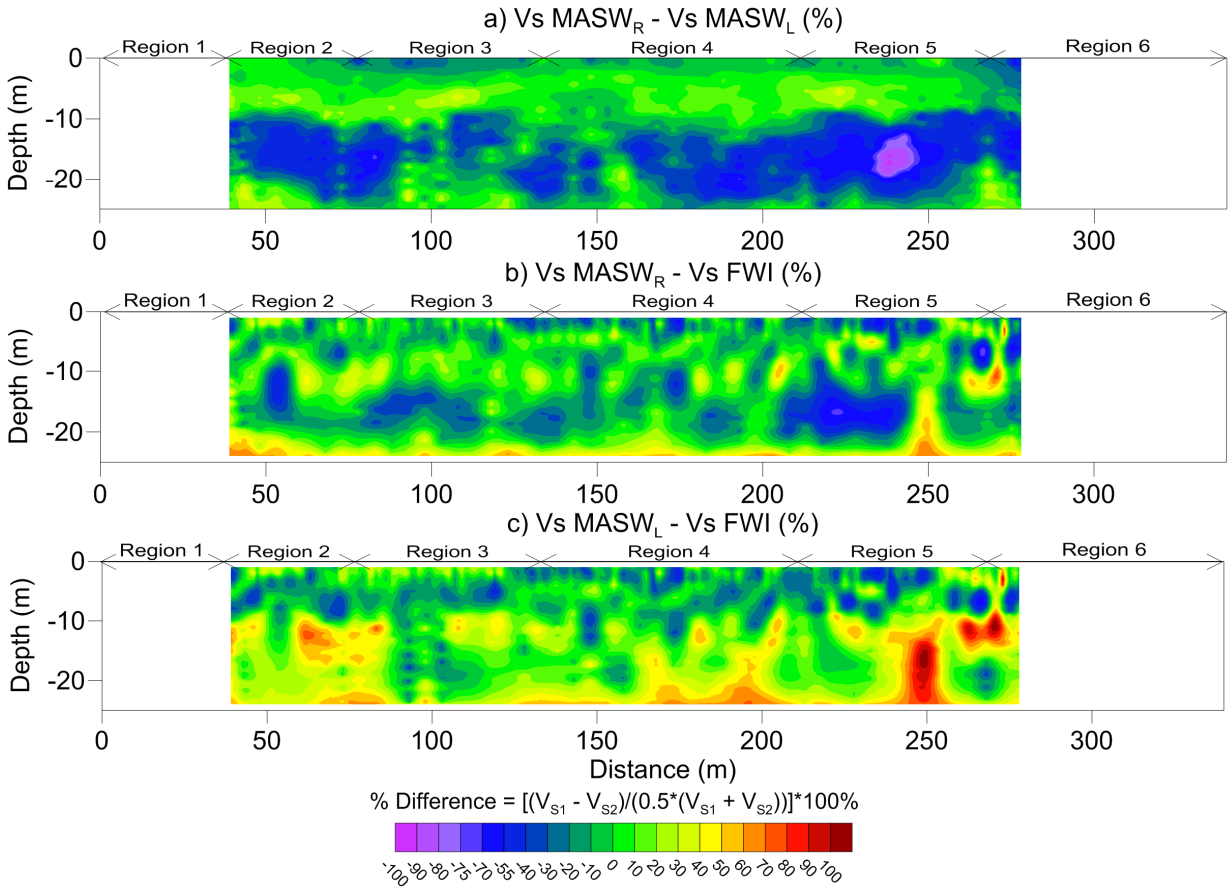

Figure 3-3. Crest percent difference plots for a) Rayleigh and Love inversions, b) FWI and Rayleigh inversions, and c) FWI and Love inversions.

Overall, surface wave methods seem most appropriate for determining the general stiffness and layering at a location, rather than detecting small features. The discrepancies in the surface wave data are likely a combination of resolution limitations and uncertainty in the inversion process. In practice, vertical resolution for MASW surveys is generally twice the

receiver spacing, or in this case, two meters, putting the resulting bedrock depths within this resolution window. Similarly, the horizontal resolution for MASW surveys is usually taken to be 10% of the array length, or in this case 2.4 meters. This results in smaller, lateral features being obscured, reinforcing the conclusion that MASW is best suited to more general subsurface profiling.

The resistivity results from the ERI and CCR surveys are shown in Figure 3-1f and Figure 3-1g, respectively. In general the survey results indicate a similar three-layer system as observed in both the surface wave results and the 1969 drilling report. These three layers, in descending order, have resistivities corresponding to clays/silts, soil-filled fractured rock, and unfractured rock (Kaufman & Hoekstra, 2001), matching the soil and rock descriptions in the drilling report well. For the CCR results, a high-resistivity bedrock layer is observed at an average of 15 meters below the surface, which is 1 - 2 meters lower than the drilling report, but with a similar bedrock profile. The ERI results, conversely, show a 1 – 2 meter shallower high-resistivity layer compared to the drilling report. The primary differences between the two methods, shown in Figure 3-5 occurs within Region 4 of the curve, where the CCR results indicate bedrock is approximately 1-2 meter deeper than the drilling report, while the ERI indicates bedrock is approximately 3-4 meters higher than indicated in the drilling report. This anomaly in Region 4 was not observed in any of the surface wave results indicating the feature is likely not related to a major change in stiffness in the region. However, the region could be related to seasonal water level variations like those documented by Inazaki and Hayashi (2011) and may represent internal erosion that has occurred in that region. Given the CCR survey was completed following a wet and cold winter, on March 16, 2016, whereas the ERI survey was completed during a warm summer, on June 22, 2015, some variations in the resistivity values

would be expected due to temperature, but the majority of the difference is likely due to a difference in the quantity of water present in the area during each survey. If internal seepage were occurring through the region, this would result in the removal of fines from the region, and promote more rapid changes in the water content in the region as the water elevation in Kinion Lake changed. In the resistivity results, this would manifest itself as lower resistivity values when water levels are higher (higher water content) and higher resistivity values when water levels are lower (lower water content) due to the inability of the bedrock on retain the ground water when the lake level drops in drier months. This seems increasingly likely when comparing the specific and relative resistivity differences, as seen in Figure 3-5. The resistivity values in the shallow clay layer from the March survey are higher than those in the June survey, likely due to temperature (Sjödahl, et al., 2008; Rein, et al., 2004), while those in the middle and bedrock layers are much lower, indicating less water content in the top two layers in the summer. The effects of temperature and recent precipitation are likely sources for the very shallow (<=1m) resistivity differences, for example, Rein et al. (2004) found that within the top 0.25 m of the surface, temperature effects can result in 20% differences in resistivity measurements. Finally, this internal erosion is supported by the approximate surface elevation of the lake outlet (7-10 meters below the crest of dam), which corresponds to the depths at which this highly variable restivity zone occurs. The detection of potential internal erosion based on seasonal differences highlights the necessicity of resistivity monitoring or at least the use of multiple surveys in different seasons for determining seepage issues. The variance in rainfall and time of year would result in different flow rates through the dam and though Kinion Lake water levels are not regularly logged and cannot confirm this, Illinois river gage readings from Savoy, AR, shown in Figure 3-4 show higher water levels both immediately preceding and in the months (especially

January) leading up to the OhmMapper testing performed in March than for the ERI testing performed in mid-June.

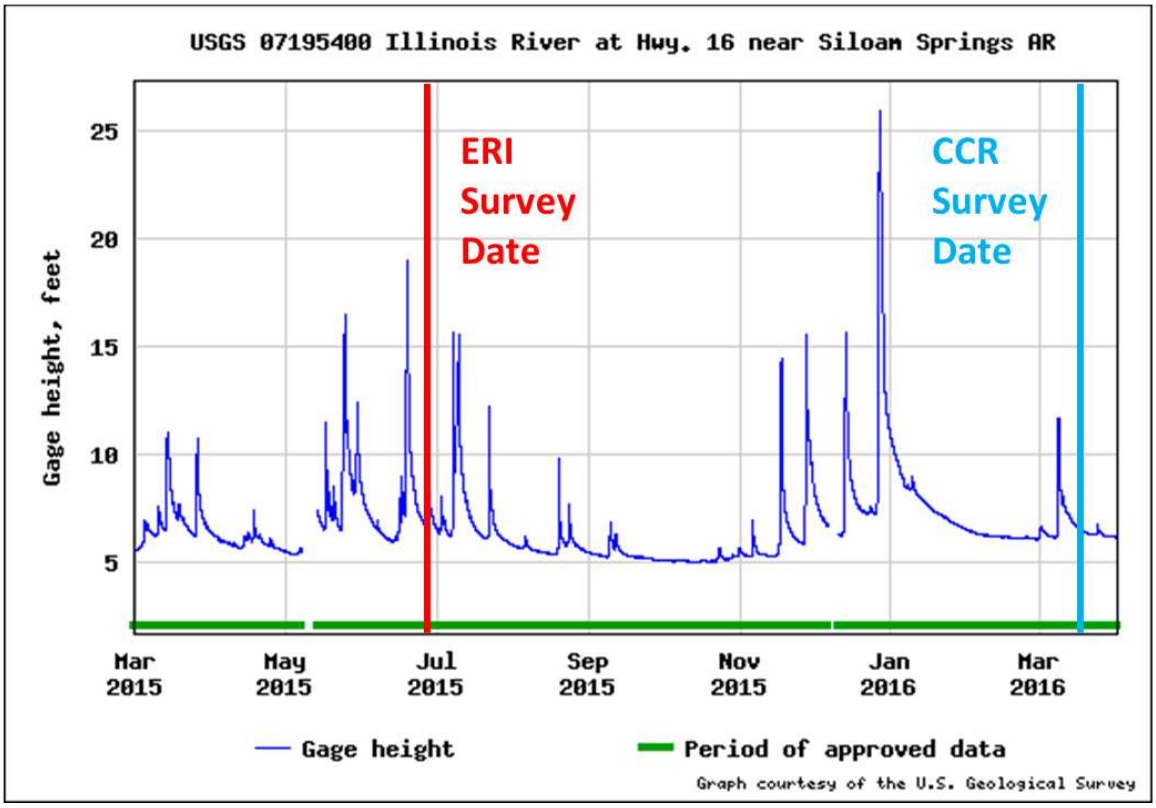

Figure 3-4. USGS river gauge readings for the year between resistivity tests at Siloam Springs, AR.

Comparing the resistivity and Vs results, the primary differences between the methods are the depths at which layers are resolved in the subsurface, though each method is typically within 1 – 2 meters of the depths determined using the drilling report. This depth variability is likely due to the complex geology, specifically the second transition layer, which the drilling investigation found very difficult to distinguish from the bedrock. This transition layer combined with seasonal variations and resolution limitations inherent to the methods used likely lead to the variations observed in the data. Seasonal precipitation variations and potential internal erosion are likely responsible for the OhmMapper results over-estimating (to deep) bedrock depth

relative to the drilling report and the ERI results under-estimating (to shallow) the bedrock depth. Overall, the use of multiple resistivity tests in different seasons seems very useful for detecting this transition layer and the potential internal erosion for the dam.

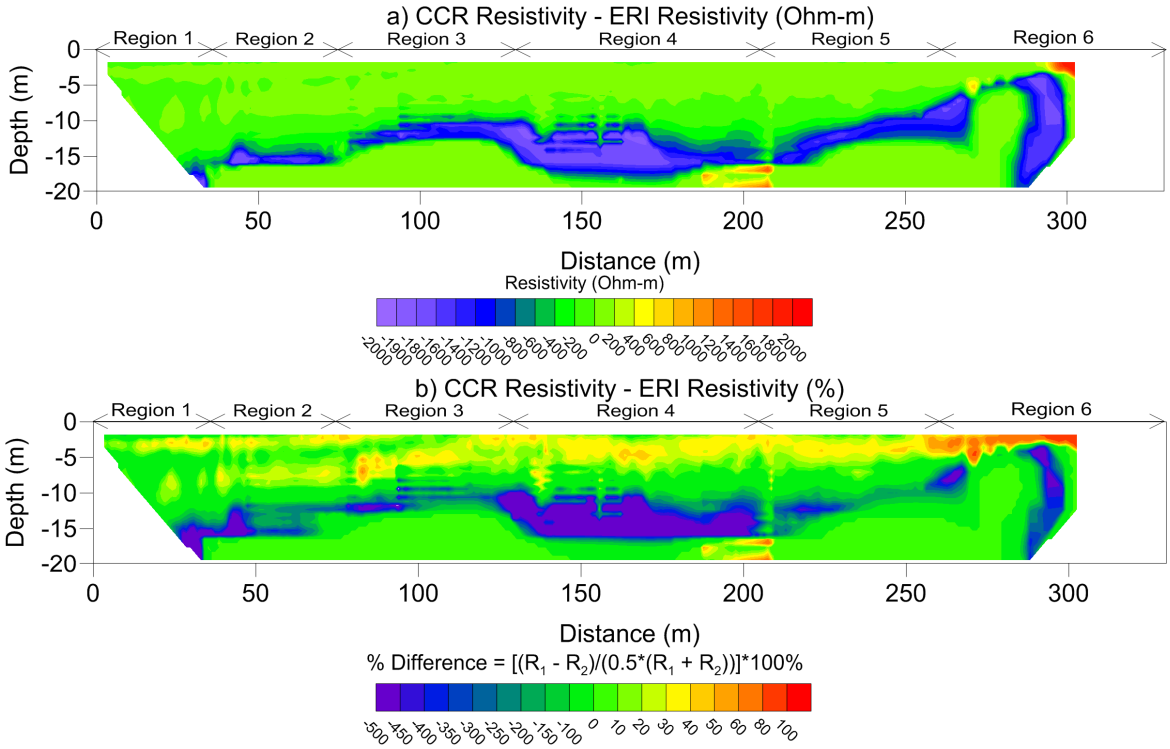

Figure 3-5. Actual (Ohm-m) and relative (%) resistivity differences between the OhmMapper and ERI profiles along the crest.

3.2 Toe

The downstream toe of Kinion Lake Dam was the most extensively tested location in and effort to detail the more complex subsurface layering and features (see Figure 2-1b). The results of a single survey line for the Love wave dispersion velocity profile (Figure 3-6a), $MASW_L$ Vs profile (Figure 3-6b), and the CCR and ERI profiles in Figures 3-6c and 3-6d, respectively. Although traditional $MASW_R$ was conducted along the same line, the results, shown in Figure 3-6, were of very poor quality. Example dispersion curves from the $MASW_L$ and $MASW_R$ are shown in Figure 3-7a and 20b, respectively. The Love wave dispersion curve has a smooth high

quality fundamental mode trend, while the Rayleigh wave dispersion curve has no useable trend with only small sections of the curve which potentially could be useable data. Given this very poor quality Rayleigh wave dispersion data, Love type surface waves seem much better suited to these shallow bedrock sites than Rayleigh waves. Comparing the 2D profiles in Figure 3-6, a valley type bedrock rock profile is observed for each of the methods with only the ERI line extending far enough to resolve both edges of the valley. The bedrock layer resolved in the profiles starts near the surface in Region 1, is within 5 meters of the surface in Region 2, and is quickly sloping downward, extending beyond the maximum investigation depths (7 – 10 meters) in Region 3. In addition, the resistivity results (both CCR and ERI), indicate a low resistivity zone in Region 4 from about 2 meters deep extending down to the bedrock, which could indicate an area of high water content (clays/silts) or water flow. This feature is very likely the previously documented seepage locations.

To image this subsurface valley feature in more detail, 2D horizontal profiles of resistivity extending from 1 meter to 6.7 meters below the surface are shown in Figure 3-8, which were created using the multiple CCR lines collected along the toe. In the plots, a bedrock layer is observed that is shallower and more resistive at the North end of the site but deeper, or at least less resistive toward the Southwest corner indicating a valley feature that extends perpendicular away from the dam. The low point of the valley (observed in Figure 3-8), is the location of the largest seep observed during large precipitation events. Based on the investigation from the dam crest, the region of suspected internal erosion in the dam (Region 4), seems to line up very well with the location the subsurface valley observed at the toe of the dam. The fairly low resistivity values in this location may indicate actual water presence or the deposition of fines from the interior of the dam.

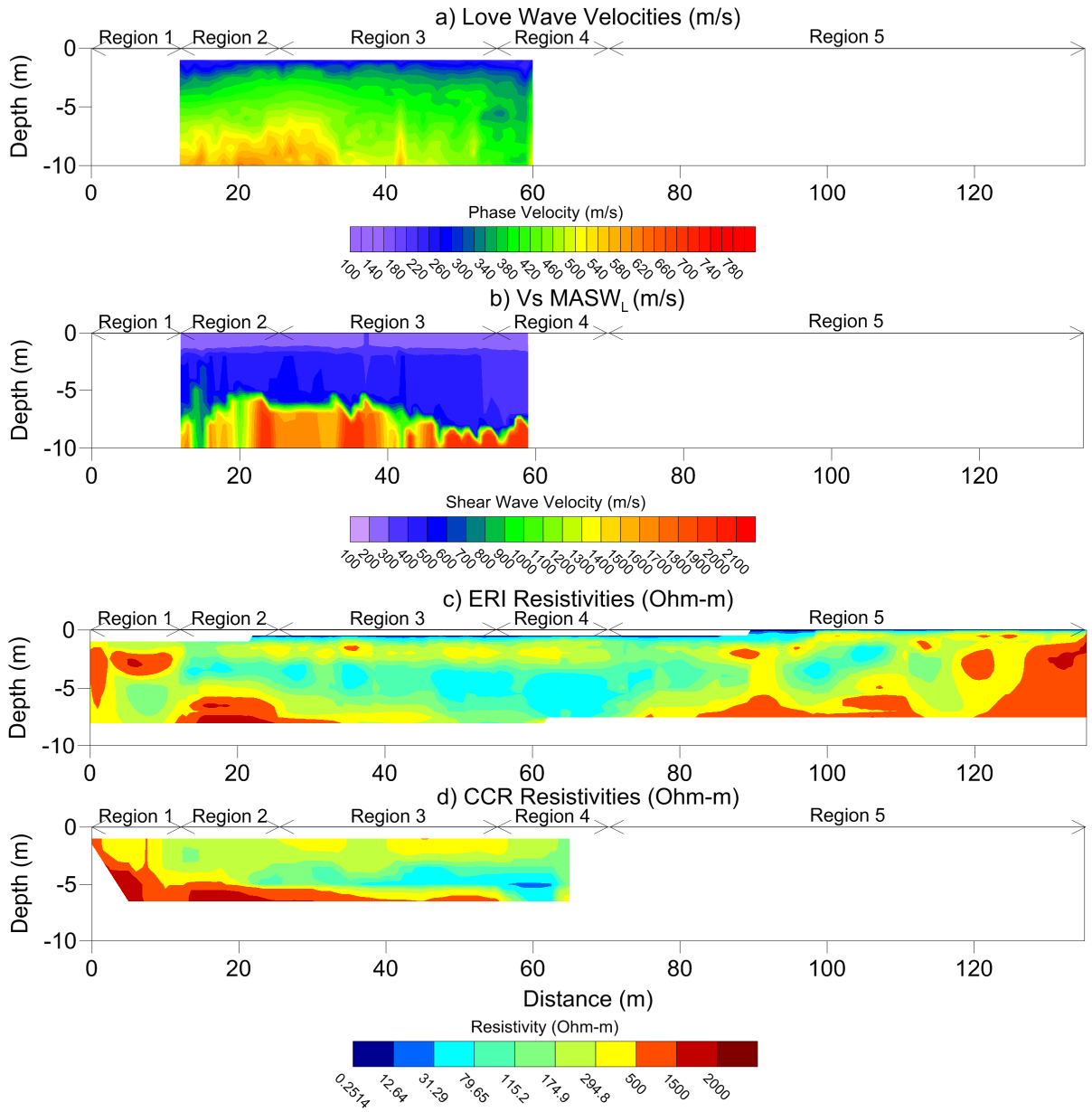

Figure 3-6. Profiles along the dry-side toe of Kinion Lake Dam: a) love wave velocities, b) shear wave velocities from the Love wave inversion, c) CCR resistivities, and d) ERI resistivities. The regions are areas of interest discussed in the text.

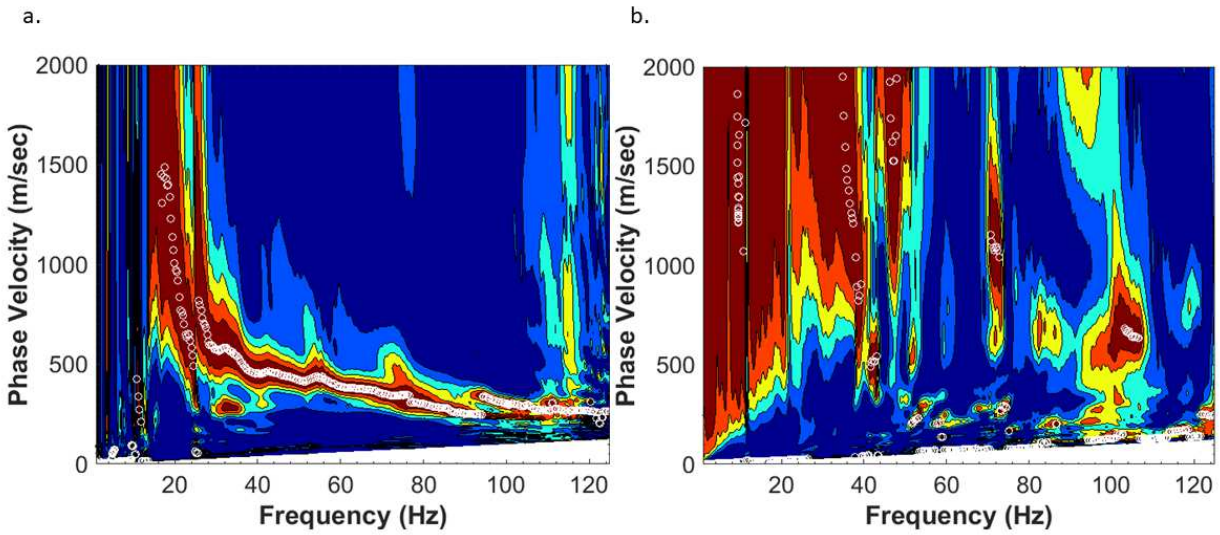

Figure 3-7. Typical a) Love wave and b) Rayleigh wave dispersion images from the toe of Kinion Lake Dam.

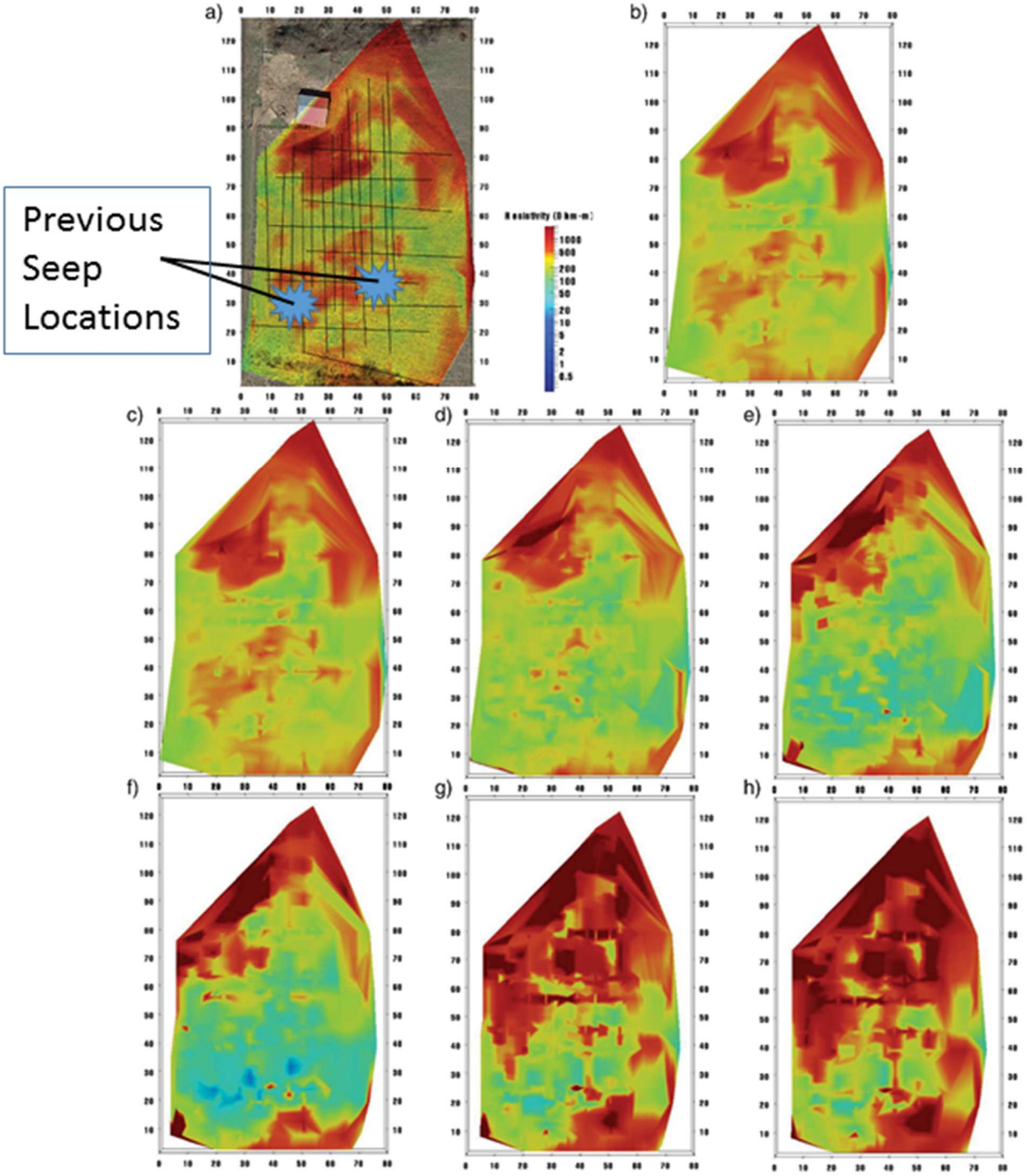

Figure 3-8. Crossections of the toe of Kinion Lake Dam at various depths: a) 0 meters with map overlay, b) -1 m, c) -2 m, d) -3 m, e) -4 m, f) -5 m, g) -6 m, h) -6.7 m.

4 Conclusions

MASW, FWI, ERI and CCR surveys were conducted along the crest and the downstream toe of Kinion Lake Dam. The bedrock layer below the dam was resolved using each of the methods within 1-2 meters of the location determined from a previous drilling program. However, the presence of a weather bedrock layer lead to some difference between the methods and ambiguity regarding the location of bedrock beneath the crest of the dam. $MASW_R$ and FWI was determined to be more effective for locations deeper bedrock (the dam itself), whereas $MASW_L$ was determined to be more effective for locations with shallow and complex bedrock (along the toe). An area of potential internal erosion was observed along the southern edge of the dam (around 130 – 210 meters along the survey lines). The detection of this erosion was possible by comparing resistivity profiles made in different seasons (wet versus dry seasons), corresponding to different water levels in Kinion Lake. A subsurface valley feature was also imaged along the downstream toe of the dam perpendicular to the region of potential internal erosion in the dam. The deepest point in the valley was also the location of the large seep that occurs along the downstream toe during large precipitation events. The location of these regions could be a seepage channel which promotes internal erosion of the dam.

5 References

ASCE, 2013. *Minimum Design Loads for Buildings and Other Structures.* ASCE/SEI 7-10 ed. Reston: American Society of Civil Engineers.

ASCE, 2013. *Minimum Design Loads for Buildings and Other Structures.* ASCE/SEI 7-10 ed. s.l.:American Society of Civil Engineers.

ASCE, 2017. *Dams | ASCE's 2017 Infrastructure Report Card.* [Online] Available at: http://www.infrastructurereportcard.org/wp-content/uploads/2017/01/Dams-Final.pdf

ASCE, 2017. *Levees | ASCE's 2017 Infrastructure Report Card.* [Online]
Available at: http://www.infrastructurereportcard.org/wp-content/uploads/2017/01/Levees-Final.pdf

Asch, T., Deszcz-Pan, M., Burton, B. & Ball, L., 2008. *Geophysical characterization of American river levees, Sacramento, California, using electromagnetics, capacitively coupled resistivity and dc resistivity,* Reston: U.S. Geological Survey.

Asch, T., Deszcz-Pan, M., Burton, B. & Ball, L., 2008. *Geophysical characterization of American river levees, Sacramento, California, using electromagnetics, capacitively coupled resistivity and dc resistivity,* s.l.: U.S. Geological Survey.

Baines, D. et al., 2002. Electrical resistivity ground imaging (ERGI): a new tool for mapping the lithology and geometry of channel-belts and valley-fills. *Sedimentology,* June, 49(3), pp. 441-449.

Ben-Menahem, A. & Singh, S. J., 1981. *Seismic Waves and Sources.* New York City: Springer-Verlag.

Bolt, B., 1993. *Earthquakes.* New York City: W.H. Freeman.

Cardarelli, E., Cercato, M. & De Donno, G., 2014. Characterization of an earth-filled dam through the combined use of electrical resistivity tomography, P- and SH-wave seismic tomography and surface wave data. *Journal of Applied Geophysics,* April.pp. 87-95.

Cox, B. & Wood, C., 2011. *Surface Wave Benchmarking Exercise: Methodologies, Results and Uncertainties.* Georisk 2011, Atlanta, ASCE, pp. 845-852.

Cox, B. & Wood, C., 2011. *Surface Wave Benchmarking Exercise: Methodologies, Results and Uncertainties.* s.l., s.n., pp. 845-852.

Dahlin, T., 1996. 2D resistivity surveying for environmental and engineering applications. *First Break,* July, 14(7), pp. 275-283.

Foster, M., Fell, R. & Spannagle, M., 2000. The statistics of embankment dam failures and accidents. *Canadian Geotechnical Journal,* 37(5), pp. 1000-1024.

Foti, S., Lai, C. G. R. G. J. & Strobbia, C., 2015. *Surface Wave Methods for Near-Surface Site Characterization.* Boca Raton: CRC Press.

Garman, K. & Purcell, S., 2004. Applications for Capacitively Coupled Resistivity Surveys in Florida. *The Leading Edge,* 23(7), pp. 697-698.

Hayashi, K. & Konishi, C., 2010. *Joint Use of a Surface-wave Method and a Resistivity Method for Safety Assessment of Levee Systems.* GeoFlorida 2010, Atlanta, ASCE, pp. 1340-1349.

Hayashi, K. & Konishi, C., 2010. *Joint Use of a Surface-wave Method and a Resistivity Method for Safety Assessment of Levee Systems.* s.l., s.n., pp. 1340-1349.

Heisey, J. & Stokoe II, K. M. A., 1982. Moduli of Pavement Systems from Spectral Analysis of Surface Waves. *Transportation Research Board,* pp. 22-31.

Inazaki, T. & Hayashi, K., 2011. *Utilization of Integrated Geophysical Surveying for the Safety Assessment of Levee Systems.* SAGEEP 2001, Charleston, SEG.

Inazaki, T. & Hayashi, K., 2011. *Utilization of Integrated Geophysical Surveying for the Safety Assessment of Levee Systems.* Charleston, s.n.

Inazaki, T. & Sakamoto, T., 2005. *Geotechnical Characterization of Levee by Integrated Geophysical Surveying.* Proceedings of the International Symposium on Dam Safety and Detection of Hidden Troubles of Dams and Dikes 2005, Xi'an, China, CHINCOLD.

Inazaki, T. & Sakamoto, T., 2005. *Geotechnical Characterization of Levee by Integrated Geophysical Surveying.* s.l., s.n.

Johansson, S. & Dahlin, T., 1996. Seepage monitoring in an earth embankment dam by repeated resistivity. *European Journal of Engineering and Environmental Geophysics,* 1(3), pp. 229-247.

Kaufman, A. & Hoekstra, P., 2001. *Electromagnetic Soundings.* Oxford: Elsevier Science & Technology.

Loke, M., 1999. *Electrical Imaging Surveys for Environmental and Engineering Studies: A Practical Guide to 2-D and 3-D Surveys.* San Jose: http://www.geometrics.com.

Loke, M. & Barker, R., 1996. Rapid least-squares inversion of apparent resistivity pseudosections by a quasi-Newton method Normal access. *Geophysical Prospecting,* January.pp. 131-152.

Love, A., 1911. *Some Problems of Geodynamics.* London: Cambridge University Press.

Love, A., 1927. *A Treatise on the Mathematical Theory of Elasticity.* Cambridge: Cambridge University Press.

McNeill, J., 1980. *Electromagnetic Terrain Conductivity Measurement at Low Induciton Numbers,* Ontario: Geonics Limited.

Min, D.-J. & Kim, H.-S., 2006. Feasibility of the surface-wave method for the assessment of physical properties of a dam using numerical analysis. *Journal of Applied Geophysics,* July, 59(3), pp. 236-243.

Mofarraj, B., 2017. *Laboratory Resistivity Measurements for Soil Characterization,* Fayetteville, AR: University of Arkansas.

Mohamed, A. M., Abu El Ata, A., Azim, F. A. & Taha, M., 2013. Site-specific shear wave velocity investigation for geotechnical engineering applications using seismic refraction and 2D multi-channel analysis of surface waves. *NRIAG Journal of Astronomy and Geophysics,* Volume 2, pp. 88-101.

Nazarian, S. & Stokoe II, K. H., 1983. *Evaluation of Moduli and Thicknesses of Pavement Systems by Spectral-Analysis-of-Surface-Waves Method,* Washington: Transportation Research Board.

NRCS, 2011. *Geophysical Study Muddy Fork Site 1 Near Prairie Grove, AR,* Little Rock: Natural Resources Conservation Service.

NRCS, 2011. *Geophysical Study Muddy Fork Site 1 Near Prairie Grove, AR,* LIttle Rock: Natural Resources Conservation Service.

NRCS, 2016. *ERI Report, Muddy Fork Site 1 (Kinion Lake Dam), Washington County, Arkansas,* Little Rock, AR: NRCS.

NRCS, 2016. *ERI Report, Muddy Fork Site 1 (Kinion Lake Dam), Washington County, Arkansas,* Little Rock, AR: NCRS.

Oldenborger, G., Pugin, A.-M. & Pullan, S., 2013. Airborne time-domain electromagnetics, electrical resistivity and seismic reflection for regional three-dimensional mapping and characterization of the Spiritwood Valley Aquifer, Manitoba, Canada. *Near Surface Geophysics,* pp. 63-74.

Palacky, G., 1987. Clay Mapping Using Electromagnetic Methods. *First Break,* 5(8), pp. 295-306.

Panthulu, T., Krishnaiah, C. & Shirke, J., 2001. Detection of seepage paths in earth dams using self-potential and electrical resistivity methods. *Engineering Geology,* November, Volume 59, pp. 281-295.

Park, C. B., Miller, R. D. & Xia, J., 1999. Multichannel Analysis of Surface Waves. *Geophysics,* May-June, 64(3), pp. 800-808.

Pellerin, L., Groom, D. & Johnston, J., 2003. *Multi-receiver OhmMapper survey over a former fuel tank site.* 9th EAGE/EEGS Meeting, Houten, 2003, EAGE.

Pellerin, L., Groom, D. & Johnston, J., 2003. *Multi-receiver OhmMapper survey over a former fuel tank site.* s.l., s.n.

Rein, A., Hoffman, R. & Dietrich, P., 2004. Influence of natural time-dependent variations of electrical conductivity on DC resistivity measurements. *Journal of Hydrology,* 15 January, 285(1-4), pp. 215-232.

Rix, G. J., Stokoe II, K. H. & Roesset, J. M., 1991. *Experimental Study of Factors Affecting the Spectral-Analysis-of-Surface-Waves Method,* Washington: Transportation Research Board.

Samyn, K. et al., 2014. Integrated geophysical approach in assessing karst presence and sinkhole susceptibility along flood-protection dykes of the Loire River, Orléans, France. *Engineering Geology,* Volume 183, pp. 170-184.

Sapia, V. et al., 2017. Multidisciplinary geophysical approach to map a disposal site: The Ponza island case study. *Journal of Applied Geophysics,* pp. 264-274.

SCS, 1970. *Investigation of Structure Deficiency: Foundation Drilling and Grouting Muddy Fork of Illinois River Watershed - Site No. 1,* Little Rock: NRCS.

SCS, 1970. *Investigation of Structure Deficiency: Foundation Drilling and Grouting Muddy Fork of Illinois River Watershed - Site No. 1,* s.l.: Soil Conservation Service.

Seaton, W. J. & Burbey, T. J., 2002. Evaluation of two-dimensional resistivity methods in a fractured crystalline-rock terrane. *Journal of Applied Geophysics,* August, 51(1), pp. 21-41.

Sjödahl, P., Dahlin, T. & Johansson, S., 2005. Using resistivity measurements for dam safety evaluation at Enemossen tailings dam in Souther Sweden. *Environmental Geology,* December, 49(2), pp. 267-273.

Sjödahl, P., Dahlin, T., Johansson, S. & Loke, M., 2008. Resistivity monitoring for leakage and internal erosion detection at Hällby. *Journal of Applied Geophysics,* Volume 65, pp. 155-164.

Strutt, J. W., 1885. On Waves Propagated along the Plane Surface of an Elastic Solid. *Proceedings of the London Mathematical Society,* November, 1-17(1), pp. 4-11.

Thomson, W. T., 1950. Transmission of Elastic Waves through a Stratified Soil Medium. *Journal of Applied Physics,* 21(89), pp. 89-93.

Timofeev, V., Rogozinski, A., Hunter, J. & Douma, M., 1994. A New Ground Resistivity Method for Engineering and Environmental Geophysics. *Symposium on the Application of Geophysics to Engineering and Environmental Problems 1994,* pp. 701-715.

Tran K.T. and Luke B. 2017. Full Waveform Tomography to Resolve Desert Alluvium. *Soil Dynamics and Earthquake Engineering*, Vol. 9, pp. 1-8, DOI: 10.1016/j.soildyn.2017.04.018.

Tran K.T., McVay. M., Faraone M., and Horhota D. 2013. Sinkhole detection using 2-D full seismic waveform tomography. *Geophysics;* 78 (5): R175–R183.

Tran K. T. and McVay M. 2012. Site characterization using Gauss-Newton inversion of 2-D full seismic waveform in time domain. *Soil Dynamics and Earthquake Engineering*; 43: 16-24.

U.S. Army Corps of Engineers, 2000. *Design and Construction of Levees,* Washington: USACE.

U.S. Army Corps of Engineers, 2004. *General Design and Construction Considerations for Earth and Rock-Fill Dams,* Washington: USACE.

U.S. Army Corps of Engineers, 2016. *NID National.* [Online]
Available at: http://nid.usace.army.mil/cm_apex/f?p=838:5:0::NO

Vireux J. and Operto S. 2009. An overview of full-waveform inversion in exploration geophysics: Geophysics; 74(6): WCC1-WCC26.

Wang, G. et al., 2016. Layered internal structure and breaching risk assessment of the Higashi-Takezawa landslide dam in Niigata, Japan. *Geomorphology,* 15 August, Volume 267, pp. 48-58.

Wathelet, M., 2008. An improved neighborhood algorithm: Parameter conditions and dynamic scaling. *Geophysical Research Letters,* May.35(9).

Wood, C., Ellis, T. & Teague, D. C. B., 2014. *Comprehensive Analysis of the UTexas1 Surface Wave Dataset.* Geo-Congress 2014, Atlanta, ASCE, pp. 820-829.

Zywicki, D. J. & Rix, G. J., 1999. *Frequency□Wavenumber Analysis of Passive Surface Waves.* SAGEEP 1999, Tulsa, SEG, pp. 75-84.

Zywicki, D. J. & Rix, G. J., 1999. *Frequency□Wavenumber Analysis of Passive Surface Waves.* s.l., s.n., pp. 75-84.

Zywicki, D. J. & Rix, G. J., 2005. Mitigation of Near-Field Effects for Seismic Surface Wave Velocity Estimation with Cylindical Beamformers. *Journal of Geotechnical and Geoenvironmental Engineering,* August, 131(8), pp. 970-977.